# Chapter 5: Geochemistry

## INTRODUCTION

This study represents the first systematic geochemical investigation of the Boggabri Volcanics. Previously available data are restricted to a single analysis of pitchstone (Jensen, 1907), a few analyses from a bentonite deposit (Saint-Smith, 1912; Raggatt, 1924; Loughnan and See, 1959) and analyses of a rhyolite and a dacite obtained during metalliferous mineral exploration (Schmidt, 1988). Data available are essentially restricted to major elements. The pitchstone of Jensen (1907) was notable for its high water content (10.05%) and because it was subsequently cited by Johannsen (1932) in his encyclopaedic review of igneous petrology. Brownlow and Arculus (1993) presented preliminary results from this study. Vickers (1991, 1993) and Moody et al. (1991, 1993) inferred similarities to the Early Permian Werrie Basalt and Halls Peak volcanics respectively based on comparison with data produced early in this investigation.

Forty five of the fifty registered samples (see Petrology chapter for definitions and nomenclature) have been analysed by conventional XRF and INAA techniques and for Loss on Ignition (see Appendix 1 for techniques, Table A1.1–4 and Fig. A1.1 of Appendix 1 and Fig. 7 for analyses and sample locations). Of these forty five samples, twelve are select Boggabri Volcanics ($SFBR_{04}$, $SED_{05}$, $SMPR_{06}$, $SLPR_{08}$, $SFA_{09}$, $SOA_{10}$, $SOB_{12}$, $SLPR_{13}$, $SAD_{24}$, $SFBR_{25}$, $SLPR_{29}$, and $SPB_{39}$), thirty are altered Boggabri Volcanics (#1–#3, #7, #11, #14–#20, #22, #26, #28, #30–#38, and #40–#45) and three are unassigned volcanics (#21, #23, #27). All analysed rhyolitic pitchstones are included among select Boggabri Volcanics.

Fig. 24 summarises symbols used herein on geochemical diagrams (see also Fig. A2.1 in Appendix 2).

## COMPOSITIONAL RANGE AND TRENDS

The Boggabri Volcanics compositional range is systematically described and illustrated in Appendix 2. Cr (as an immobile proxy for Mg) and $SiO_2$ are used therein as variation indices. Several simply defined trends are discussed therein, including the Main Trend (comprising a Mafic Segment among more mafic rocks, an Intermediate Segment, and a

## Select Boggabri analyses

| | |
|---|---|
| ■ | Olivine basalt (SOB $_{12}$) |
| ● | Olivine-poor basalt (SPB $_{39}$) |
| ◆ | Olivine-free andesite (SOA $_{10}$) |
| ▶ | Olivine andesite (SFA $_{09}$) |
| ✳ | Augite dacite (SAD $_{24}$) |
| ◀ | Enstatite dacite (SED$_{05}$) |
| ▼ | Biotite rhyolite lava (SFBR $_{04}$) |
| ▲ | Pyroxene rhyolite lava ( SLPR$_{06}$, SLPR$_{08}$, SLPR$_{29}$) |
| ◈ | Biotite rhyolite ignimbrite (SFBR $_{25}$) |
| ◈ | Pyroxene rhyolite ignimbrite (SFBR $_{13}$) |

## Trend lines

| | |
|---|---|
| ---------- | Main Trend |
| ·········· | Cross Trends 1 and 2 |
| ·········· | Dyke Trend |

## Altered Boggabri rocks

| | |
|---|---|
| □ | Olivine basalt (#14, #41) |
| ○ | Basalt (#11, #33, #38, #43, #44, #45) |
| ◇ | Basaltic andesite (#03) |
| ▷ | Andesite (#15, #20, #42) |
| ◁ | Dacite (#07, #16, #17, #18, #19, #26, #30, #35, #36, #40) |
| ▽ | Biotite rhyolite (#32) |
| △ | Pyroxene rhyolite #01, #02, #22, #28, #29, #31, #34, #37) |

## Alteration styles

| | |
|---|---|
| ○ | Pitchstones (SFBR $_{04}$, SMPR $_{06}$, SLPR$_{08}$, SFBR $_{25}$, SLPR$_{29}$) |
| × | Carbonated (#03, #07, #11, #44) |
| + | Al-rich (#33, #40) |
| ◇ | White rhyolite #28, #32, #34, #37) |
| □ | Silicified (01, #02, #18, #22, #30, #31, #43, #45) |

Letter symbols used on Figs 26 and 27:

bs = basalt, ba = basaltic andesite, an = andesite, dc = dacite, rh = rhyolite, tbs = trachybasalt, bta = basaltic trachyandesite, ta = trachyandesite, tr = trachyte, ph = phonolite, pa = pantellerite

Fig. 24: Symbols used on geochemical diagrams (Figs 25–27).

Felsic Segment among more felsic rocks), two Cross Trends linking mafic and intermediate compositions, and an anomalous Dyke Trend amongst intermediate compositions. These trends, while simplistic in concept, are useful both as a frame of reference on many diagrams and as a prompt for subsequent analysis of fractionation and mixing trends.

**Cr v $SiO_2$** and **$TiO_2$ v Zr** (Fig. 25) encapsulate four of the more common variants of the Main Trend that are documented systematically in Appendix 2. Firstly, Cr displays a large range in the Mafic Segment but only minor (systematic) ranges at lower levels in the Intermediate and Felsic segments; MgO and some trace elements exhibit broadly similar patterns although there is considerable variation in abundance levels at the Mafic Inflection. Secondly, $SiO_2$ exhibits negligible increase in the Mafic Segment but a substantial increase in the Intermediate Segment and a lesser increase in the Felsic Segment. Thirdly, $TiO_2$, increases significantly in the Mafic Segment but decreases throughout the Intermediate and Felsic segments; $Fe_2O_3$t, MnO, $P_2O_5$ and many trace elements behave similarly, except for minor increases in the Felsic Segment for some. Fourthly, Zr shows a substantial increase through the Mafic and Intermediate segment to a peak at about the Felsic Inflection, but a substantial decline in the Felsic Segment; $Na_2O$ and some trace elements follows a broadly similar pattern. Most select Boggabri Volcanics plot along or close to the Main Trend. Altered Boggabri Volcanics are more scattered, but many plot near the Main Trend or are offset in a way predictable from the style of alteration and from immobile element patterns (see Appendix 2).

Some analyses plot systematically away from the Main Trend, and closer to Cross Trend 1 (#45) or to Cross Trend 2 ($SOA_{10}$) for some element. $SAD_{24}$ also plots off the Main Trend for many elements, especially HFSE (see Dyke Trend on Figs A2.2–A2.30). Correspondence with these trends for other elements is mediocre due to alteration or to uncertainty in trend definitions.

## CLASSIFICATION

The IUGS classification of major volcanic rock types is based primarily on the Total Alkali Silica (**TAS**) diagram (Le Maitre et al., 1989; Cox et al., 1979). Mobility of alkalis and silica is a major challenge in applying the IUGS classification to altered volcanic rocks and LeMaitre et al., 1989) explicitly recommend caution in applying that scheme to volcanic rocks with > 2% $H_2O$. Alternative proposals mainly use 'immobile' elements (P, Ti, Ga or Ce) or ratios (Zr/Ti, Zr/$P_2O_5$, Ga/Sc, Nb/Y) to replace total alkalies as an indicator of alkalinity, or silica as a fractionation index (e.g., Floyd and Winchester, 1975; Winchester and Floyd, 1977). Notable amongst these are **Zr/$TiO_2$ v Nb/Y, Ga/Sc v Nb/Y** and **$SiO_2$ v Zr/$TiO_2$** (Winchester and Floyd, 1977).

Classification of volcanic series is more controversial, especially in the distinction of

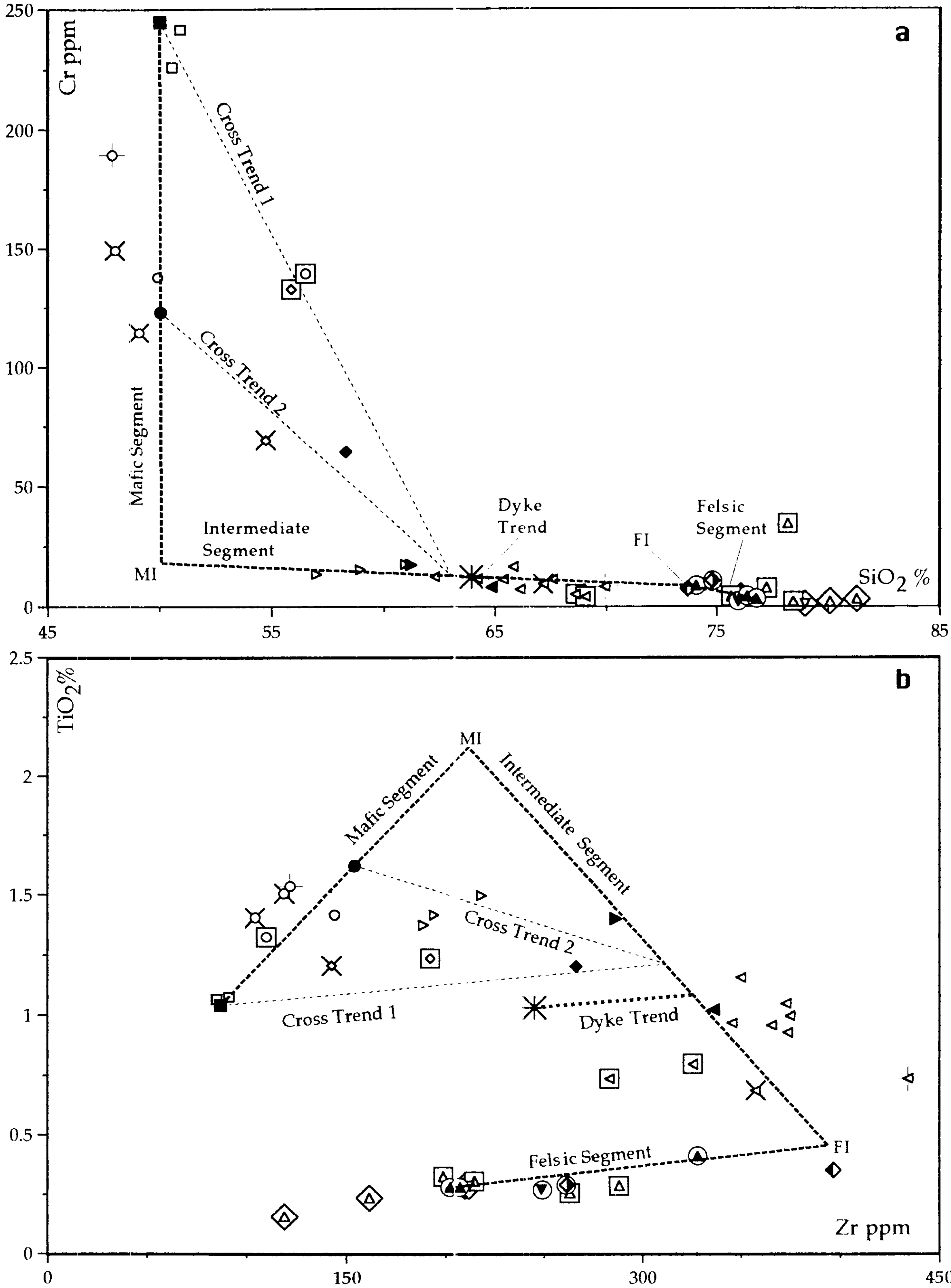


**Fig. 25 (a–b):** Representative trends and compositional ranges among Select and altered Boggabri Volcanics. See Fig. A2.1 for symbols and text for explanation. FI = Felsic Index, MI = Mafic Index.

tholeiitic and calc-alkaline series. The IUGS TAS diagram implicitly separates the alkaline from sub-alkaline (calc-alkaline and tholeiitic) rock series, and thereby largely replaces the early graphic distinctions of MacDonald and Katsura (1966), Kuno (1966), Irvine and Baragar (1971). Early iron-enrichment characterises the tholeiitic series. This series has traditionally been distinguished from the calc-alkaline series using the AFM diagram (Nockolds and Allen, 1953). More recent alternatives are **FeOt/MgO v $SiO_2$** (Miyashiro, 1974) and **Al-Fe+Ti-Mg** (Jensen, 1976; Jensen and Pyke, 1982). Middlemost (1975) distinguished the tholeiitic series from the calc-alkali (and high alumina) series using **A.I. (alkali index) v $Al_2O_3$** and distinguishes the potassic series from the sodic series using **$K_2O$ v $Na_2O$**. IUGS rock series classification uses the potassium-silica diagram (LeMaitre et al., 1989; Peccerillo and Taylor, 1976) to distinguish the shoshonitic, high-K, medium-K, and low-K series. These series do not correspond exactly with traditional terminology, but tholeiitic rocks are generally low-K and calc-alkaline are generally medium to high-K. **Molecular (Ca + K + Na)/Al v molecular (K + Na)/Al** distinguishes various levels of alumina saturation implicit in peralkaline, metaluminous and peraluminous compositions (Shand, 1950).

## TAS Classification of Boggabri Volcanics

On **TAS** (Fig. 26a, b), select Boggabri Volcanics plot in the basalt and rhyolite fields, and on the along the boundary of the andesite and trachyandesite fields, and of the dacite and trachyte fields. The Boggabri Volcanics Main Trend projects from the basalt field into the trachybasalt field then along the lower limit of the trachyandesite and trachyte fields and into the rhyolite field. Altered Boggabri Volcanics are more scattered than select rocks, and generally plot below the Main Trend in the basalt-andesite and rhyolite ranges, and above the Main Trend in the trachyte range. #33 (zeolitised basalt) plots in the trachybasalt field.

## Immobile Element Classification of Boggabri Volcanics

On **$Zr/TiO_2$ v Nb/Y** (Fig. 26e–f), the Main Trend shows a decline in Nb/Y in the Mafic Segment, a substantial increase in $Zr/TiO_2$ and a moderate increase in Nb/Y in the Felsic Segment. Select analyses plot along the Main Trend, except of some scatter among select rhyolites, especially in Nb/Y. $SAD_{24}$ is a notable exception, with significantly higher Nb/Y than the trend equivalent. Altered samples mimic the distribution of their select analogues, but show greater scatter especially in Nb/Y and a trend to higher Nb/Y. Overall, Boggabri Volcanics mostly exhibit a marginally sub-alkaline compositional spectrum ranging from basalt to rhyodacite or rhyolite (Winchester and Floyd, 1977). Only one sample with anomalously low Y has Nb/Y of greater than 1 (moderately

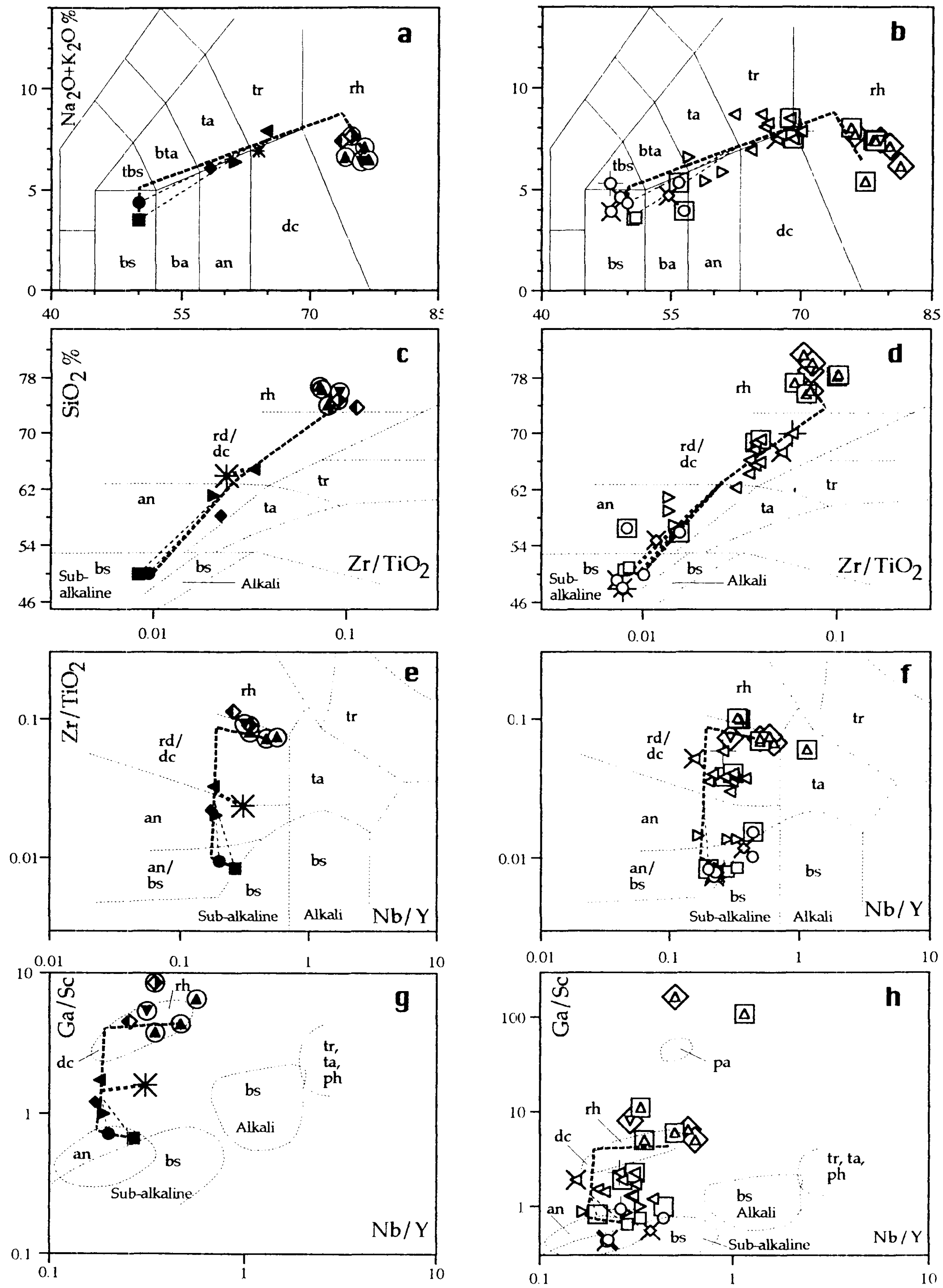


**Fig. 26:** Classification of Select (left Column) and altered (right column) Boggabri Volcanics based on: (a–b) Total Alkalis-Silica diagram; (c–e) various immobile elements. See Fig. 24 for symbols and text for explanation.

alkaline — Winchester and Floyd, 1977).

On Ga/Sc v Nb/Y (Fig. 26 g–h), the Main Trend comprises a very short Mafic Segment, a longer positively sloping Intermediate Segment, and a slightly shorter, nearly flat Felsic Segment. Select rocks plot close to the Main Trend except for a trend to higher Ga/Sc among select rhyolites and higher Nb/Y in $SAD_{24}$. Altered Boggabri Volcanics mimic this trend, except for greater scatter mainly in Ga/Sc. However, carbonated basalts and basaltic andesite are anomalous (high CaO and high Sc), and plot at higher Ga/Sc. Overall, Boggabri volcanics mostly exhibit a marginally sub-alkaline compositional spectrum ranging from basalt to rhyodacite or rhyolite (Winchester and Floyd, 1977).

On **$SiO_2$ v $Zr/TiO_2$** (Fig. 26 c–d), the Main Trend comprises a nearly flat Mafic Segment, a steep positive trending Intermediate Segment that is anomalous in being slightly bent, and a short steep, negative trending Felsic Segment. Select rocks closely mimic this trend apart from some scatter among select rhyolites. Altered rocks also follow the Main Trend, but with notably greater scatter, especially among some basalts and andesites. The slope on this trend is consistent with a marginally sub-alkaline compositional spectrum ranging from basalt to rhyodacite or rhyolite (Winchester and Floyd, 1977). This diagram shows most scatter parallel to $SiO_2$.

Analogous plots involving $Zr/P_2O_5$ instead of $Zr/TiO_2$, and plots of $Zr/TiO_2$ v Ce or Ga (not plotted) also indicate a marginally sub-alkaline compositional spectrum ranging from basalt to rhyodacite or rhyolite. These plots display marginally greater scatter than do the illustrated plots.

## Boggabri Volcanics Series Classifications

Fig. 27a–f summarises series classification for the Boggabri Volcanics.

On **$K_2O$ v $SiO_2$** (Fig. 27a–b), select basalts, andesites, $SAD_{24}$ and one select rhyolite ignimbrite ($SFBR_{25}$) plot in the medium-K field, whereas one select rhyolite plots in the low-K field, and $SMPR_{06}$ and the remaining select rhyolites plot in the high-K field. The Mafic Segment plots near the lower margin of the medium-K field, the Intermediate Segment plots obliquely across the field, and the Felsic Segment trends into the high-K field. Most altered basalts and andesite plot in the medium-K field, whereas altered dacites and rhyolites straddle the medium-K and high-K fields. In addition, one dacite (#16) plots in the shoshonitic field, and one silicified basalt and two silicified rhyolites plot in the low-K field.

On **FeOt/MgO v $SiO_2$** (Fig. 27c–d), select basalts, andesites and dacites mainly plot along the boundary of the tholeiitic and calc-alkaline fields, whereas select rhyolites

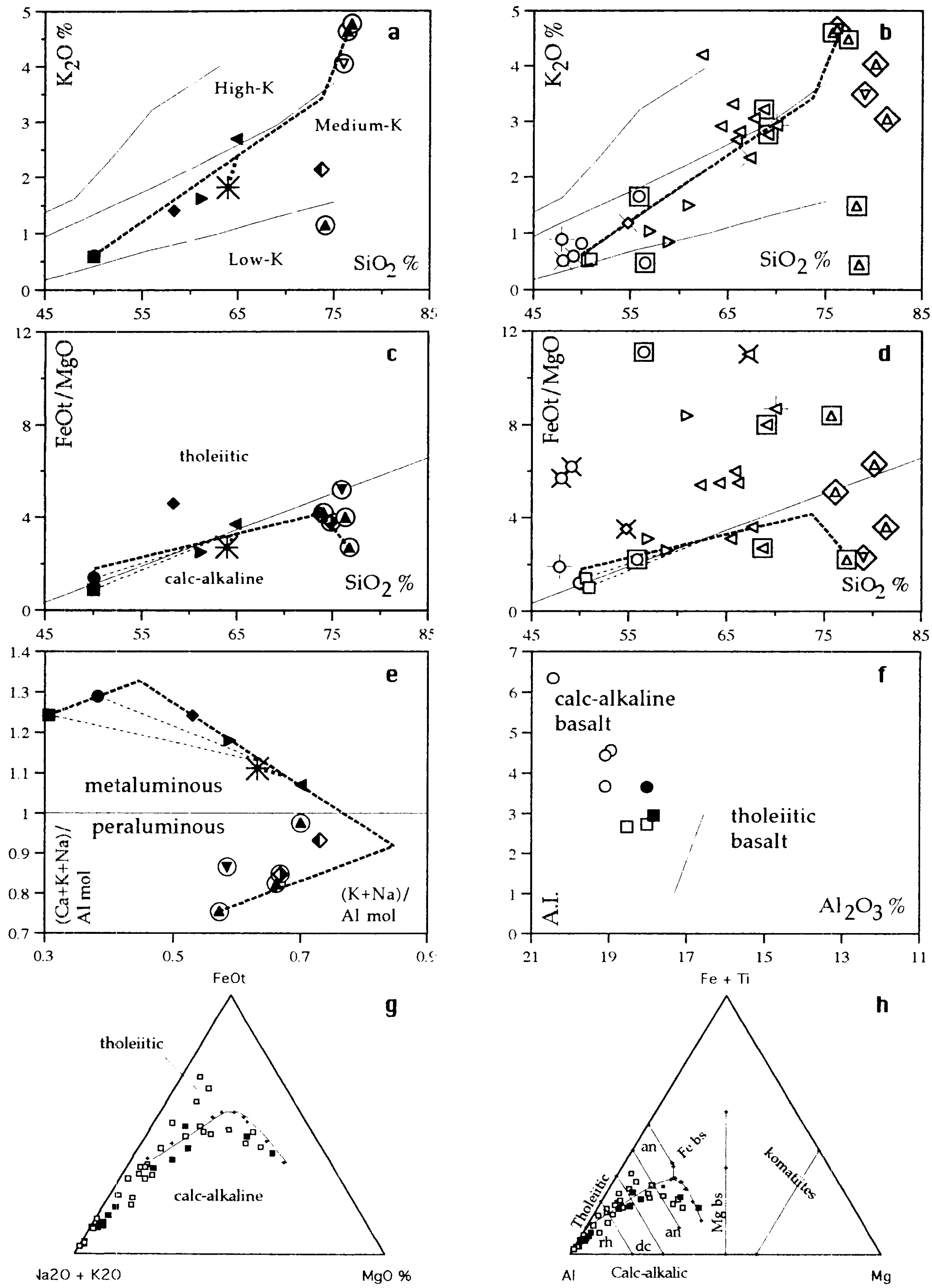


**Fig. 27:** Boggabri Volcanics series classification. (a–b) K-Si diagram for Select and altered Boggabri Volcanics respectively; (c–d) Tholeiitic v Calc-alkali series for Select and altered Boggabri Volcanics respectively; (e) Metaluminous v peraluminous for Select Boggabri Volcanics; (f) Calc-alkali v tholeiitic basalts; (g) AFM diagram; (h) Al-Fe+Ti-Mg diagram. See Fig. 1 for symbols, text for explanation.

mainly plot in the calc-alkaline field. Among select rocks, only $SOA_{10}$ with low MgO, plots obviously within the tholeiitic field. In contrast, altered rocks mainly plot with the tholeiitic field. Only one silicified rhyolite, one silicified basalt and two white rhyolites plot in the calc-alkaline field.

On **(Ca + K + Na)/Al mol v (K + Na)/Al mol** (Fig. 27e), select Boggabri Volcanics basalts, andesites and dacites are metaluminous whereas select rhyolites are peraluminous.

On **A.I. v $Al_2O_3$** Fig. 27f), select Boggabri Volcanics basalts plot within the calc-alkaline field, and well outside the tholeiitic field.

On **AFM** (Fig. 27g), all select Boggabri Volcanics except $SOA_{10}$ (with low MgO) plot within the calc-alkaline field. Most altered rocks also plot within the calc-alkaline field, but a number of rocks with low Mg (the low Mg array on **MgO v $SiO_2$** — q.v.) plot within the tholeiitic field.

On **Al-Fe+Ti-Mg** (Fig. 27h), select Boggabri Volcanics mainly plot in the calc-alkaline field, whereas some altered rocks with low Mg plot (including $SOA_{10}$) within the tholeiitic field. In additional, $SOB_{12}$ plots marginally within the High-Mg Tholeiitic field.

## Volatiles

The high water content in most select rhyolites warrants their labelling as 'pitchstones' (see Appendix 2).

## Summary

**TAS** indicates alkali contents roughly equal to the boundary between alkaline and sub-alkaline fields and a lithological range for Boggabri Volcanics from basalt to rhyolite (or their alkaline equivalents). High water contents make these classifications suspect. Immobile element plots and **$Zr/TiO_2$ v $SiO_2$** display coherent, igneous-like trends with only modest scatter mainly among rhyolite pitchstones and altered rocks (greatest scatter in Nb/Y). These broadly validate the compositional range displayed on TAS.

Other diagrams indicate the following series: medium-K series for select basalt-dacite spectrum and high-K series for select rhyolites (on **$K_2O$ v $SiO_2$**), transitional tholeiitic to calc-alkaline for most fresh rocks but tholeiitic for most altered rocks (on **FeOt/MgO v $SiO_2$**); calc-alkaline for select basalts on **A.I. v $Al_2O_3$**; calc-alkaline for most rocks and ranging to tholeiitic for one select rock and for altered rocks with low MgO (on **AFM and Al-Fe+Ti-Mg**); metaluminous for select basalts, andesites and dacites but peraluminous for select rhyolites on mol (Ca+K+Na)/Al v $SiO_2$; and outside the peralkaline field throughout the Boggabri Volcanics range on **mol (K + Na)/Al v $SiO_2$.**

Conventional terminology for sub-alkaline rocks will be used herein for simplicity and because is appropriate for most select rocks. The term 'pitchstone' is applied to most select rhyolites.

## ELEMENT ABUNDANCE SPECTRA

Normalising a series of elements in an analysis to a common reference composition and graphing it as an X-Y line graph is a powerful means of comparing geochemical analyses because such diagrams explicitly display elemental abundances and implicitly display elemental rations. This procedure is now widely practised, for example, Masuda-Coryell diagrams with C1 chondrite-normalised REEs and Mantle- or MORB-normalised 'spiderdiagrams' (Rollinson, 1993).

Such diagrams are used herein to compare $SOB_{12}$ with various geochemical reservoirs (e.g., Rollinson, 1993) and geochemical reference compositions, and to illustrate the internal variation across the Boggabri Volcanics spectrum by comparing select analyses to $SOB_{12}$. The resulting diagrams effectively summarise both elemental abundances and petrogenetically significant ratios among select Boggabri Volcanics, and thereby serve to summarise the systematic analysis of major and trace elements in Appendix 2 (Figs. A2.2–A2.30) and REE, Discriminants and Petrologically Significant Ratios in Appendix 3 (Figs. A3.1–A3.3)

### Comparisons with Major Geochemical Reservoirs

Fig. 28a–d compares relationship between $SOB_{12}$ and various geochemical reservoirs and reference compositions whose abundances have been illustrated element by element in Figures A2.2–30 of Appendix 2.

**$SOB_{12}$/C1 chondrite** (Fig. 28a) is enriched ≈ 10x HREE, increasing to ≈ 50x for La and slightly lower for Th (43 x). Ba (112 x) and Sr (120x) form notable peaks, whereas, Rb, K, Pb, and P form conspicuous troughs. Note that Rb, K and Pb would all have been volatile and partly lost as celestial dust during terrestrial accretion and P is siderophile and therefore would have been preferentially partitioned into the Earth's core (Ringwood, 1975, Taylor and McLennan, 1985). Another notable feature is a Zr-Hf-Sm anomaly comprising a small peak for Sm and trough for Hf relative to Zr (cf McDonough and Sun, 1995).

**$SOB_{12}$/pyrolite** (Fig. 28a) exhibits a similar underlying pattern in the Th-Lu range as to C1 chondrite normalised $SOB_{12}$ but at a lower level. Thus $SOB_{12}$ increases gradually from 3.6x pyrolite for Lu, 12.9x for P, 18x for La and 15.6x for Th, and exhibits a similar

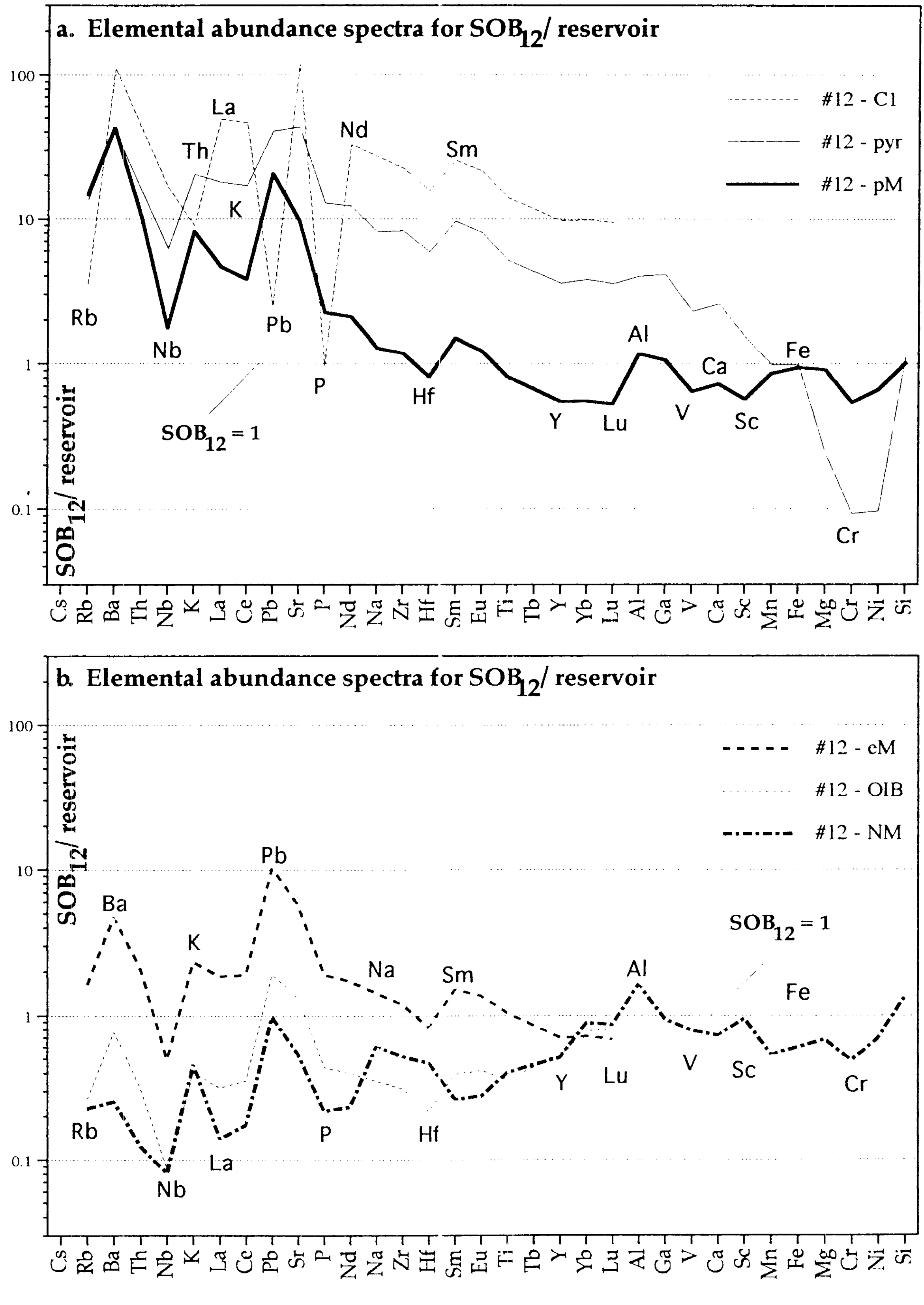


**Fig. 28 (a–b):** Elemental abundance spectrum for $SOB_{12}$ normalised to various geochemical reservoirs. (a) C1 chondrites, pyrolite, Primitive MORB; (b) E-MORB, OIB, Hawaiian Nepheline Melilitite.

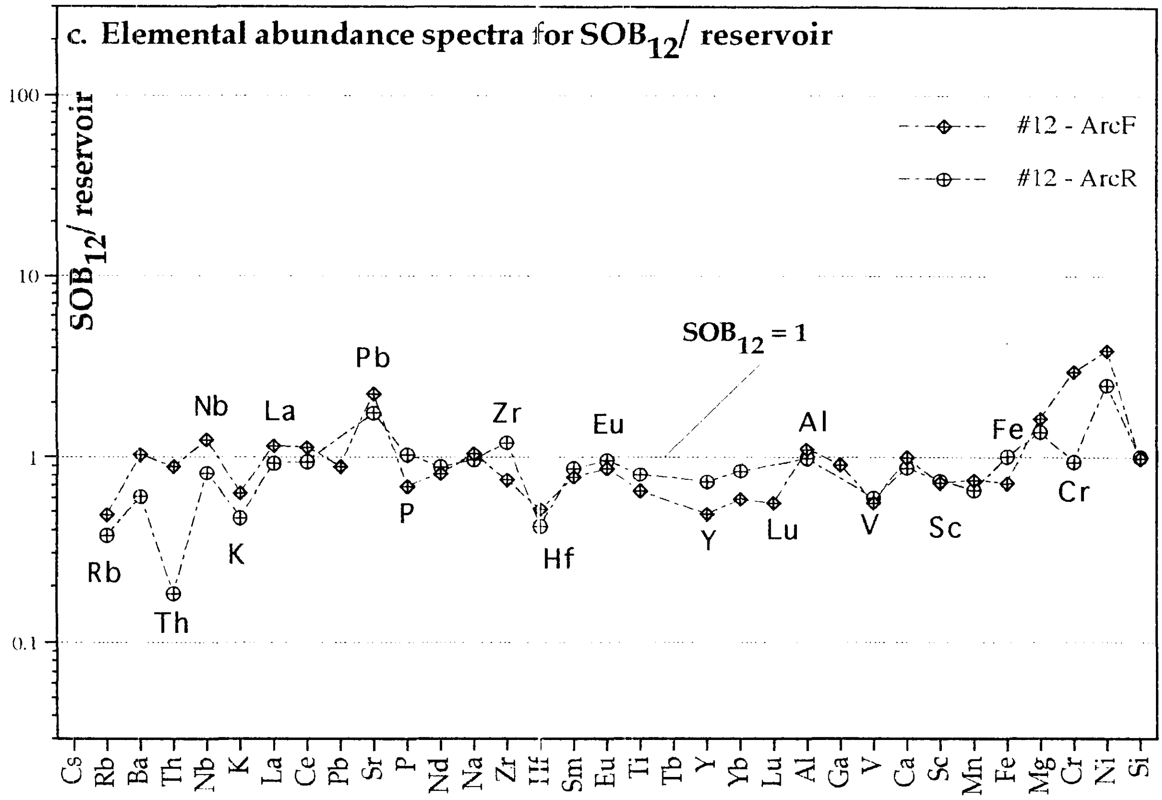


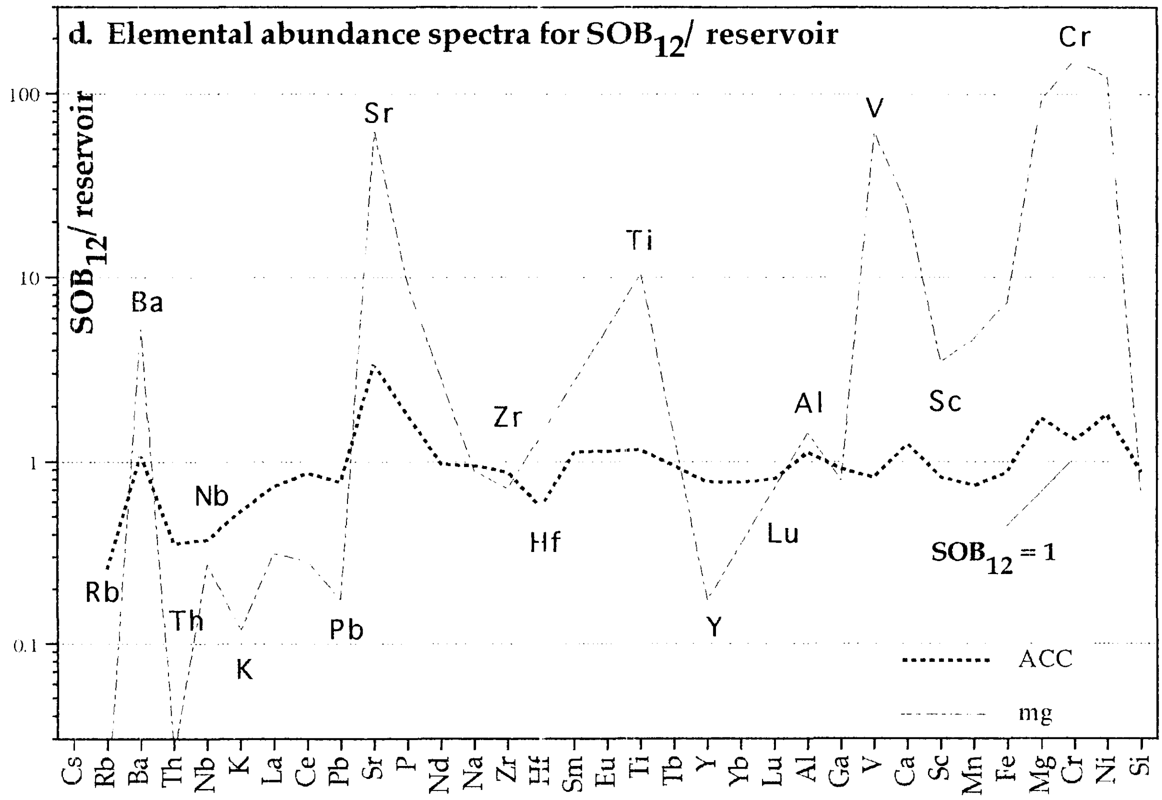


**Fig. 28 (c–d):** Elemental abundance spectrum for $SOB_{12}$ (cont.). (c) Fuji basalt (ArcF) and Rindjani basalt (ArcR); (d) Average Continental Crust (ACC) and Mole Granite (mg).

Zr-Hf-Sm anomaly as well as peaks at Ba (41x) and Sr (44x). However, the pattern of peaks and troughs from Rb to Nd is generally different, with a conspicuous trough at Nb (6.2 x) and peak at Pb (41x), but only a subdued trough at Rb (13.7x), and no anomaly at K (20.3x) or P (12.9x). The most prominent feature or the Lu-Si range is strong downward trend through V (2.3x), Sc (1 5 x), Fe (0.99x), Mg (0.24x) and Cr (0.09) then a rise through Ni and Si at 1.1 x. This trend is marked by slight peaks at Al and Ga (4.1x) and Ca (2.6x) and a slight low at Mn (0.99x).

**$SOB_{12}$/Primitive MORB** (Fig. 28a) also displays a similar underlying pattern but at a lower level for elements more incompatible than Al. Thus there is an underlying ('intermediate') trend rising from 0.55x for HREE to 2.25x for P to 4.7 x for La. However this pattern projects further to include Th at 10.3x and Rb at 14.6x. A second underlying ('lower') trend is apparent, connecting HREE to Hf at 0.82x and Nb at 1.76x Primitive MORB. A further difference compared to the pyrolite trend is a higher Ba peak (43x), a small peak for K (8.2x), a higher peak at Pb (21.5x). The Zr-Hf-Sm anomaly is also present, but with Zr slightly below the primary trend. At the compatible end of the spectrum, V, Sc, Cr and Ni are only slightly above HREE, whereas Al (1.17x) and Ga form a prominent peak and Mn, Fe, and Mg (0.92x) form a slightly lower peak.

**$SOB_{12}$/E-MORB** (Fig. 28b) follows a similar pattern to Primitive MORB, but with a gentler slope for the lower trend in incompatible elements. The Zr-Hf-Sm anomaly is also present.

**$SOB_{12}$/OIB** (Fig. 28b) also displays a broadly similar pattern of peaks and troughs to $SOB_{12}$/Primitive MORB, but superimposed on a lower trend that slopes to lower values among more incompatible elements. The Zr-Hf-Sm anomaly is also present, although slightly masked by a positive Eu anomaly.

**$SOB_{12}$/Hawaiian Nepheline Melilitite** (Fig. 28b) is broadly similar to $SOB_{12}$/OIB in the Rb-Lu range, apart from three critical differences: (a) the Zr-Hf-Sm anomaly is strikingly different with Hf significantly higher compared to Sm and slightly higher compared to Zr; (b) the intermediate trend through La, P and MREE virtually coincides with the lower trend through Nb, Sm (instead of Hf) and HREE; (c) Ba, Pb and Sr form more subdued peaks; and (d) K is more conspicuous. In addition, among more compatible elements, Ga is less prominent, Sc forms a small peak rather than a low, and there is a subdued Mn-Fe-Mg anomaly in place of the hump on $SOB_{12}$/Primitive Mantle.

**$SOB_{12}$/Fuji basalt** (Fig. 28c) displays a weakly curved, concave upward profile that is lowest at Y (0.49x) but equal to unity at Ba and Si. Peaks and troughs are subdued compared to most other patterns in Fig. 28, and include a broad, peak for Mg-Cr-Ni (Ni = 3.87), a distinct peak for Sr (2.23x), and lesser peaks for Nb, La-Ce, Na, Eu, Al-Ga, and Ca, and as well as lows for Rb (0.48), K, P and Hf (0.52). The Hf low is part of a Zr-Hf-

Sm anomaly.

**$SOB_{12}$/ArcR** (Fig. 28c) displays a broadly similar, but flatter pattern with a less pronounced low at Y (0.73). Many peaks and troughs are similar to **$SOB_{12}$/Fuji basalt,** but the Mg-Cr-Ni peak is replaced by lesser peaks at Fe and Ni (Cr = 1x), the hafnium anomaly has a different shape (Zr > Sm), there is no low at P, but there is a prominent low at Th (0.18x). In addition, there is a weak downward trend with increasing incompatibility among very highly incompatible (e.g., Nb at 0.82x).

**$SOB_{12}$/Average Continental Crust** (Fig. 28d) displays a pattern similar to **$SOB_{12}$/ E-MORB** between Sr and Lu, but slightly flatter and more subdued. Minor differences in this range include slightly higher Lu (0.8) and a slight positive Ti anomaly. Note the absence of P data. However, among more incompatible elements, the shape is considerably different, apart from a Ba peak, due the absence of Pb, K and Nb anomalies. The compatible end of the spectrum broadly overlaps **$SOB_{12}$/pM,** but not all peaks and troughs coincide.

**$SOB_{12}$/Mole Granite** (Fig. 28d) displays a strikingly different pattern from those above, made more so by the absence of many data (e.g., Ti and Y are the only available data between Zr and Al). The main features are extreme peaks for Ba, Sr (63x), Ti (10.4x), V-Ca (62x for V) and Mg-Cr-Ni (124x for Cr) and minor peaks for Nb and Al, as well as extreme lows for Rb (0.014x), Th (0.025x) and Y (0.17x), and Sc-Mn-Fe (3.46x for Sc) and lesser lows for K, Zr (no Hf data), Pb, and Ga. The pattern between Ba and Sr (lows for Th, K and Pb compared to LREE and the high for Nb) is essentially complementary to that of **$SOB_{12}$/Primitive MORB**. The positive anomalies among incompatible elements are complementary to those developed among select rhyolites (except that V and Ca are more extreme)

## Boggabri Volcanics Spectrum Normalised to $SOB_{12}$

Elemental abundance spectra normalised to $SOB_{12}$ (Fig. 29 a–b) further illustrate the various trends established in systematic analysis to the select Boggabri Volcanics spectrum (Appendix 2). Compared to $SOB_{12}$, $SPB_{39}$ shows:

- a broad enrichment in MREE and HREE (1.7x $SOB_{12}$), generally declining to negligible among more incompatible elements (Cs, Nb, La, Ce, Nd);
- small lows for Ba, K, Pb, Sr (most marked), P, and Na and a slight peak for Hf;
- progressive depletion among compatible elements (especially Cr and Ni) relative to HREE, except for a low peak at Mn and Fe (both marginally enriched); and
- $SOB_{12}$ like values for most element between Lu and Mn as well as Si, but marginal enrichment for Ga and Ca.

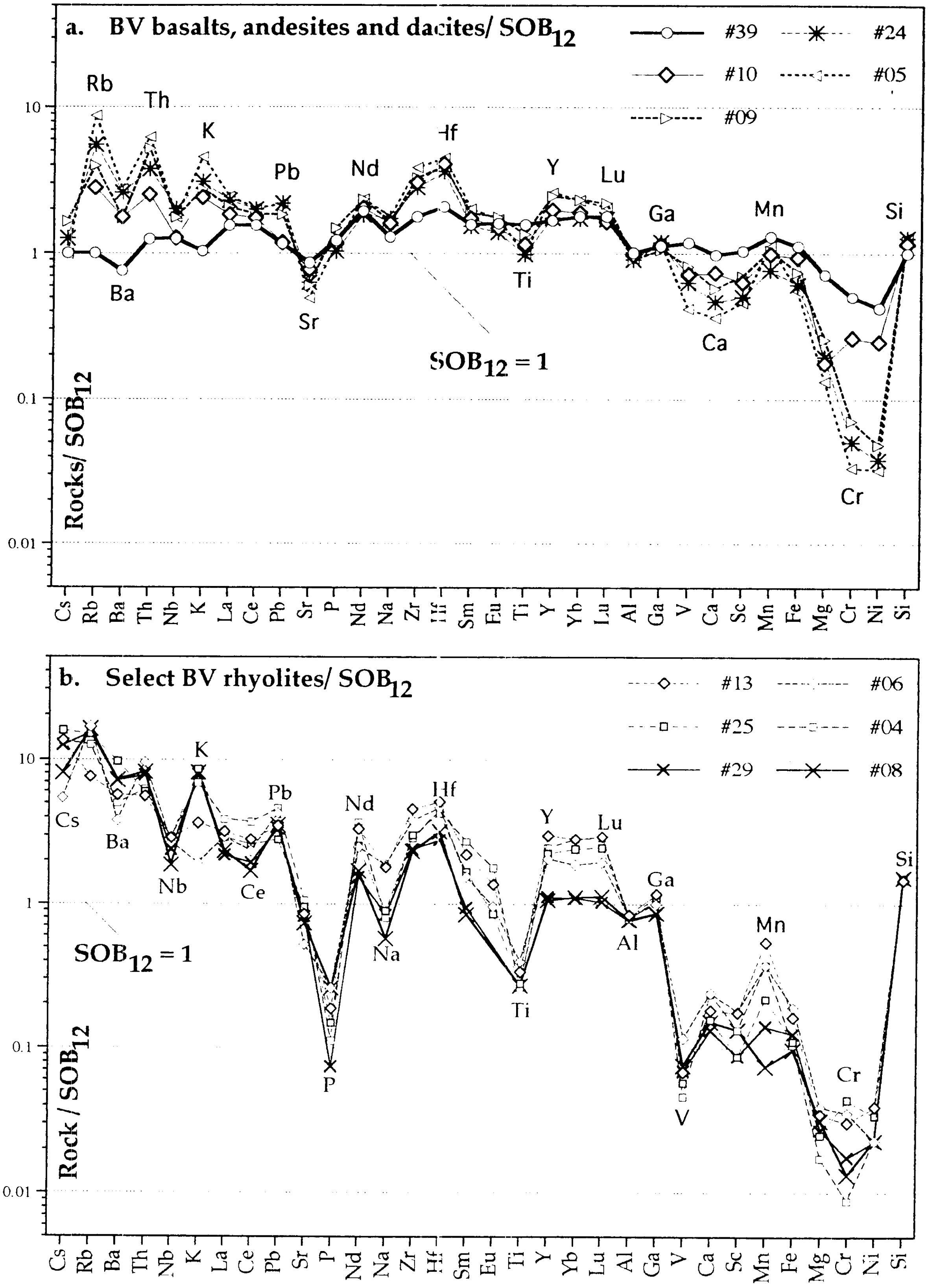


**Fig. 29:** Select Boggabri Volcanics normalised to Primitive MORB. (a) Basalts, andesites and dacites; (b) Rhyolites.

The andesite-dacite spectrum displays a similar underlying trend that is slightly higher for HREE values (up to 2.6x $SOB_{12}$ except $SAD_{24}$ with HREE ≈ $SPB_{39}$) and both higher and flatter trend for incompatible elements (Cs, Nb, Ce, Pb, Nd), but steeper and yielding progressively greater depletion among compatible elements (Ni at 0.24 to 0.03x $SOB_{12}$). Superimposed on this trend are:

- lows for Sr (also P), Na, Ti, and V-Ca-Sc;
- well developed peaks for Rb, Th, K and Zr-Hf, with the latter forming a notable hump in the middle of the spectrum;
- values for Al, Ga and Si that are respectively unchanged, slightly enriched (increasing Ga/Al), and marginally enriched compared to $SPB_{39}$;
- erratic behaviour for some elements;
- relative depletion for $SAD_{24}$ compared to $SED_{05}$ in HREE (values = $SPB_{39}$) and in incompatible elements; and
- values for HFSEs in $SOA_{10}$ that are commonly closer to $SED_{05}$ than to $SPB_{39}$.

Rhyolites systematically display more extreme behaviour, affecting both the underlying trend and peaks, including greater enrichment for incompatible elements (Rb 16.6x $SOB_{12}$) and greater depletion among compatible elements (Cr at <0.01x $SOB_{12}$). Other differences include:

- similar enrichment to $SED_{05}$ among HREE and MREE (2-3x $SOB_{12}$) for low-Si rhyolites ($SMPR_{06}$ and $SLPR_{13}$) and biotite rhyolites ($SFBR_{25}$ and $SFBR_{04}$), but significantly less enrichment for high-Si pyroxene rhyolites ($SLPR_{29}$ and $SLPR_{08}$);
- a higher base level among certain incompatible elements (Cs, Ba, Nb, La, Ce) that rises with increasing incompatibility among elements more incompatible than Pb;
- greater depletion among compatible elements, especially Cr (<0.01x $SOB_{12}$) and the Mg-Cr-Ni group generally, so that Cr<Ni;
- development of a deep trough for P (0.07 to 0.26x $SOB_{12}$), and less pronounced troughs for Ti and V;
- greater relative depletion in Sr, Na, Ti, Al (minimally) and V, and greater enrichment of Si;
- a change of shape for the V-Ca-Sc trough with V<Sc<Ca;
- a tendency for high-Si pyroxene rhyolites ($SFBR_{25}$ and $SFBR_{04}$) to exhibit relatively low abundances of high field strength elements (Nb, REE, P, Zr, Hf, Ti) and Na than other rhyolites; and
- a tendency for the mid-spectrum Hf-Zr hump to be less pronounced than among andesites and dacites.

## BIVARIATE COMPARISONS

Table 7 summarises the relationship between the compositional range of the Boggabri Volcanics and that of various geochemical reservoirs and regional comparators used in extensive bivariate comparisons (see Appendix 2 for details and explanation).

## SUMMARY

The results of the present investigation are again broadly consistent with the few data previously available.

The Boggabri Volcanics range from basalt to rhyolite of sub-alkaline to mildly alkaline affinity. The subalkaline component is broadly calc-alkaline, but tending to transitional tholeiitic for some parameters. Basalt, andesite and dacite are medium-K and metaluminous whereas select rhyolites are high-K and peraluminous. Most select rhyolites are pitchstones due to the high water content, and are slightly altered, possibly accounting for their peraluminous character.

Element abundance spectra for $SOB_{12}$ clearly show an arc signature (Brownlow and Arculus, 1993; Appendix 2) with high $Ba_N$, $Pb_N$ and $Sr_N$, and low $Nb_N$, but only intermediate $K_N$, $Rb_N$ and $Th_N$ (atypical of arcs) using MORB-normalised data. $SOB_{12}$ also exhibits a Zr-Hf-Sm anomaly, enrichment in highly incompatible HFSE, depletion in HREE and uncommonly high Mg/Cr and high Ni/Cr. This combination is highly unusual and not reported in standard references. High $Al_2O_3$ is also indicates arc affinity, but denies all other major settings. Abundance comparisons (Appendix 2) failed to model the low Y and Hf, and high Cs in $SOB_{12}$ (Hf and Cs data are from reconnaissance analyses and require confirmation). Similarly, no widespread source for the high Mg/Cr or Ni/Cr is known. No one standard geochemical reservoir can model all other characteristics. For example, only Hawaiian Nepheline Melilitite models the Zr-Hf-Sm anomaly, but lacks an 'arc signature' and high $Al_2O_3$.

Discriminant analysis (see Appendix 3) does not yield a consistent indication of magmatic source. Petrogenetically significant ratios involving Ba (Ba/Th, Ba/La, Ba/Nb) or Nb (Rb/Nb, Th/Nb, K/Nb, La/Nb -- see Appendix 3) are generally closest to arc basalts and distinct from other mafic or continental comparators, but those involving alkalis are distinctly lower than comparable ratios involving alkaline earths (e.g., Rb/Nb or K/Nb v Ba/Nb). Zr/Nb is similar to Primitive MORB and Arc basalts; and REE ratios (La/Ce, La/Sm, Ce/Sm, La/Yb, Ce/Yb, Sm/Yb) are in the range of non-arc mafic comparators, but higher than arc basalts or Average Continental Crust (Appendix 3). Again a mixed source is indicated, possibly involving an arc signature (high Ba, less elevated Rb and K) superimposed on a combination of Primitive MORB and

# Table A2.3: Comparison of Select BV with Geochemical Reservoirs and Reference Compositions

| | Major Oxides | | | | | | | | | Trace Elements | | | | | | | | | | | | | | |
|---|---|---|---|---|---|---|---|---|---|---|---|---|---|---|---|---|---|---|---|---|---|---|---|---|
| | *Al* | *Fe* | *Ca* | *Mg* | *Na* | *K* | *Ti* | *P* | *Mn* | *Ni* | *Cu* | *Zn* | *Sc* | *V* | *Ga* | *Y* | *Zr* | *Sr* | *Pb* | *Ce* | *Nb* | *Th* | *Ba* | *Rb* |
| Arc volcanics | <> | ≈ | <= | ≈ | ≥ | <> | ≥ | ≥ | ≈ | ≈ | ≤ | ≥ | < | ≤ | ≥ | ≈ | ≥ | > | > | ≥ | ≥ | <> | <> | <> |
| CRZ volcanics | > | <= | <> | ≈ | ≥ | ≤ | ≈ | ≈ | ≈ | ≈ | <> | - | ≥ | - | ≤ | ≈ | ≈ | <> | ≈ | <> | ≤ | ≈ | < | ≈ |
| CFB volcanics | > | <= | <> | ≈ | ≥ | ≤ | ≤ | ≤ | ≤ | ≤ | - | < | ≤ | <> | ≤ | ≤ | ≤ | <> | ≈ | <> | ≤ | ≤ | ≤ | ≤ |
| OFB volcanics | > | ≤ | < | ≤ | > | > | ≥ | > | ≈ | ≤ | - | - | < | - | ≥ | ≈ | ≥ | > | > | > | ≈ | > | - | > |
| OIP tholeiitic volcanics | > | < | < | ≈ | > | ≈ | ≤ | ≥ | ≈ | - | - | - | < | - | ≈ | ≈ | ≈ | > | ≈ | ≈ | ≤ | ≈ | ≈ | ≈ |
| OIP alkalic volcanics | > | < | > | > | < | < | < | < | ≤ | - | - | - | > | - | ≤ | ≤ | ≤ | <> | ≈ | < | < | ≤ | < | < |
| Nundle Plutonic Suite | < | > | < | < | > | > | > | > | > | ≈ | ≤ | ≥ | ≤ | ≈ | ≥ | > | > | <> | <> | ≥ | > | <> | ≥ | ≥ |
| Moonbi Plutonic Suite | > | ≈ | <= | ≤ | > | < | > | ≥ | ≥ | ≤ | ≈ | ≥ | ≈ | ≈ | ≥ | <> | > | <> | ≤ | ≤ | ≤ | < | <> | < |
| Uralla Plutonic Suite | > | ≈ | <= | ≤ | > | < | > | > | > | ≤ | ≈ | ≥ | ≤ | ≈ | ≥ | ≥ | > | > | < | ≤ | ≈ | < | <> | < |
| Petroi Metabasalt | <> | ≈ | <= | ≤ | ≤ | ≤ | ≤ | < | ≈ | >< | - | - | - | ≤ | ≥ | ≈ | ≈ | > | - | ≈ | < | - | <> | ≈ |
| Werrie Basalt | ≈ | ≈ | ≈ | ≈ | ≤ | ≈ | ≈ | <> | ≈ | ≈ | ≥ | ≤ | ≈ | ≥ | ≈ | <> | ≥ | ≈ | ≥ | ≈ | ≈ | ≥ | ≈ | ≥ |
| Halls Peak volcanics | >= | <= | <= | ≤ | ≈ | ≥ | ≈ | ≤ | ≥ | ≈ | ≤ | ≤ | ≤ | ≈ | <> | ≤ | ≤ | > | ≤ | < | ≈ | < | ≥ | ≤ |
| NEO mafic complexes | ≥ | >= | < | ≤ | < | ≥ | ≥ | > | ≥ | ≈ | ≥ | ≥ | ≤ | ≥ | > | ≥ | > | > | ≥ | > | ≥ | ≈ | > | ≤ |
| Copeton Plutonic Suite | >= | <= | <= | ≤ | < | ≤ | ≥ | > | > | ≈ | < | > | < | ≈ | ≈ | > | > | > | ≤ | ≈ | ≥ | ≤ | > | < |
| Hillgrove Plutonic Suite | >= | <= | <= | ≤ | < | ≤ | ≥ | ≥ | ≥ | ≈ | <> | ≥ | ≤ | ≈ | ≈ | ≥ | > | > | ≤ | ≈ | ≤ | < | > | < |
| Late Carb. volcanics | ≈ | ≈ | ≈ | ≈ | ≤ | <> | > | > | ≥ | ≤ | ≥ | - | ≤ | ≤ | ≤ | > | > | ≈ | < | - | - | - | ≈ | <> |
| Late Carb. rhyolites | ≈ | ≈ | ≈ | ≈ | >< | <> | ≥ | ≥ | ≈ | ≈ | ≈ | ≈ | - | ≈ | <> | ≈ | ≥ | ≥ | <> | - | <> | ≤ | ≥ | ≤ |
| Late Carb. sills | ≈ | ≈ | ≈ | ≈ | ≤ | <> | > | > | ≈ | - | - | - | - | - | - | - | - | - | - | - | - | - | - | - |
| Tertiary volcanics | ≥ | ≥ | > | > | ≤ | < | <> | <> | ≥ | ≈ | ≥ | < | > | ≥ | - | ≤ | ≤ | ≥ | ≤ | < | < | ≤ | <> | ≤ |
| Unassigned volcanics | ≈ | ≈ | ≈ | > | ≤ | ≈ | ≈ | ≤ | ≥ | ≈ | ≈ | ≈ | ≤ | ≤ | ≈ | ≈ | ≈ | ≈ | < | < | ≈ | < | < | ≈ |

≈ = BV range similar to reference range

<> = BV range within large reference range

>< = BV range includes small reference range

≤ = BV values overlap lower reference range

≥ = BV values overlap upper reference range

< = BV values smaller than reference values

> = BV values larger than reference values

\- = no data available

Hawaiian Nepheline Melilitite characteristics (for most other elements).

Among regional comparisons tested (Appendix 2), the only similarity is with the Werrie Basalts, confirming earlier suggestions by Vickers (1991, 1993). The Halls Peak volcanics show far fewer similarities and some significant differences, despite similar Zr/Nb (Moody et al., 1991, 1993). Late Carboniferous volcanics, all granitoid suites, Petroi Metabasalt, and Early Permian NEO mafic complexes also differ from the Boggabri Volcanics. Too few data are available for systematic comparison with other Early Permian volcanics, but limited available data indicates possible similarity to the Warrigundi Igneous Complex (Flood et al., 1988), basal volcanic rocks of the Gunnedah Basin (Leitch et al., 1988; Leitch and Skilbeck, 1991; Leitch, 1993), Alum Mountain Volcanics (Leitch et al., 1991; Jenkins and Nethery, 1992), and probably the volcanic rocks of the northern Bowen Basin (Murray, 1990).

# Chapter 6: Synthesis

## INTRODUCTION

The Boggabri Volcanics have been investigated because they provide critical information concerning several important geological issues: (a) their internal rock relationships and implications for the structure and development of the Boggabri Ridge; (b) their age and correlation; (c) their depositional environment and implications for regional palaeogeography; (d) their compositional range and causes of variation; (e) their magmatic affinity and source; and (f) their regional geological setting and origin. Issues (a) and (d) have received most attention during this investigation.

## INTERNAL ROCK RELATIONSHIPS AND THE BOGGABRI RIDGE

### Internal Rock Relationships

The internal rock relationships within the Boggabri Volcanics are equivocal due to poor outcrop and a lack of laterally persistent marker beds. The only probable inter-domain correlation is that of the thin sediment unit in the Railway, Heathcliffe and Daisymede domains (implied by McPhie, 1984b). This correlation is critical because it would exclude significant block uplift on the Boggabri Fault (Tadros, 1993b) as a mechanism to source conglomerates in the overlying Maules Creek Formation (cf. Thomson, 1986) or the Porcupine Formation (Thomson et al., 1993) or to explain difference in the elevation of the Maules Creek Formation across the ridge (cf Tadros, 1993b). However, correlation of this horizon (implied by McPhie, 1984b) would indicate minor vertical movement on two inferred NNW trending faults now covered by the Namoi River Flood Plain (Map 1) to account for minor differences in attitude and elevation between these outcrops. However, dacites overlying the sedimentary horizon in each domain differ texturally and it is unclear whether that is significant or just due to tapping of different positions of a magma chamber. In addition, the basalt substrate to the sediments in the Railway and Heathcliffe domains contrasts with the rhyolite breccia and dacitic ignimbrite substrate in the Daisymede Domain. Neither observation negates the correlation, but sedimentation would have had to have been similar over a distance of about 3 km despite changes in volcanic rocks. More detailed evaluation of this correlation is needed.

Each of the eight domains recognised within the Boggabri Volcanics would appear to comprise a superposed sequence of volcanic rocks and minor sediments. However, soil cover prevents discounting the possible presence of cryptic, bedding-parallel thrust. Eastward thrusting of the leucocratic pyroxene rhyolite lavas and domes in the upper part of the Railway and possibly the Baan Baa domains would appear to the most likely candidate. It would also be consistent with asymmetric folding (steep W limb, flatter E limb) in a small isolated syncline keel of Leard and Maules Creek Formation in the Railway Domain near the south-western limit of Boggabri Volcanics outcrop. Such thrusting needs to be considered because it would be one of the few geometrically feasible mechanisms to source the Maules Creek Formation from the Boggabri Ridge (cf. Thomson, 1986). It would also be consistent with eastward thrusting on the Severn and Wongwibinda Thrusts in the NEO arguably at about this time (see Appendix 5). Moreover, altered basalts and rhyolite pitchstones at the bases of some rhyolite lavas would plausibly form ready slip planes during thrusting. As yet there is no specific evidence of thrusting from either a seismic survey across the ridge (Korsch et al., 1993) or from field investigations, but the hypothesis cannot yet be negated owing to inappropriate siting of the seismic line to test it, and to the presence of soil covering critical boundaries. Thrusting is less likely to be significant elsewhere owing to the complex internal geometry of the Boggabri Volcanics.

## Structure of the Boggabri Ridge

There is a crude symmetry across the Boggabri Ridge (apart from the downfaulted? Barbers Pinnacle Domain), with leucocratic pyroxene rhyolite lavas most prominent on either margin, and dacites most prominent in the middle (Fig. 7, Map 1). This implies an anticlinal structure. The broad similarity of the Baan Baa and Railway domains supports this possibility whereas the lack of detailed correlation between the Daisymede and Therribri domains does not. However, detailed petrological and volcanological examination could show that perceived differences between the two domains (mainly based on field observations) are influenced by differences in alteration, or that the differences reflect the mode of tapping one or more coeval magma chambers of similar composition. Similarly, more detailed mapping of the Southern Forest and adjacent areas is also needed to ascertain whether any of its rhyolite lavas correlate with the Northern Forest or Barbers Pinnacle domains

Overall the anticlinal model is critical because it would imply that only a few hundred metres of Boggabri Volcanics has been removed from the centre of the ridge, and therefore it would probably not have been a major source of sediment for the overlying Maules Creek Formation. Support for this argument comes from the fact that the highest outcrop of Maules Creek Formation (447 m at Leard TS in the Leard State Forest) is similar to that of the volcanics (452 m on unit Nrl1, nearby). Both localities are near then eastern outcrop margin of the Boggabri Ridge, implying that the Maules Creek Formation might once have onlapped and capped the Ridge. This was a major reason why Brownlow (1981b) did not accept the earlier suggestion of Hanlon (1949b) that the conglomerates of the Maules Creek Formation were derived from the Boggabri Ridge. This argument is also supported by the occurrence of sparse quartz-rich rhyolite clasts, unlike any rocks recognised in the Boggabri Volcanics, among the Maules Creek conglomerate pebbles sectioned by Thompson (1986).

### Synvolcanic Structures

There are two areas of probable down-faulting or sagging in the Boggabri Volcanics. Firstly the flat-lying leucocratic pyroxene rhyolite lavas of the Barbers Pinnacle Domain could be part of a caldera fill (Brownlow and Arculus, 1993), or else could have been down-faulted along a major structure that extends north-easterly and bounds the Daisymede and Southern Forest domains and then extends further to influence the straight, north-easterly trending boundary between the Boggabri Volcanics and the overlying Permian sedimentary units. (This margin is depositional, but a basement fault-controlled monocline could explain its straightness and help explain the major embayment in the boundary between the Boggabri Volcanics and the overlying sedimentary units.) An occurrence of southerly dipping lavas and ignimbrite immediately south of an inferred fault separating the Barbers Pinnacle and Southern Forest domains (i.e. dipping into the possible caldera) supports syn-volcanic downfaulting. The second area of downfaulting is the Northern Forest Domain, which has the appearance of a caldera with a southern, faulted, margin and a western, down-sagged, margin (see Field Geology chapter).

## AGE AND CORRELATION

The present investigation confirms the occurrence of lithologies in the Boggabri Volcanics that are similar to the Werrie Basalt (Carey, 1935; Vickers, 1991, 1993), the Gunnedah Volcanics and Werrie Basalt at Gunnedah (Manser, 1965a,b and detailed mapping of these volcanic rocks and the overlying equivalents of the Leard and Maules Creek formations by Brownlow, 1977b), cores of basal volcanic rocks from the subsurface Gunnedah Basin (Leitch et al., 1988; Leitch and Skilbeck, 1991; and extensive observations of then available drill cores by Brownlow, 1977b), and possibly the Warrigundi intrusives (Flood et al., 1988, and brief reconnaissance observations during this investigation). Specifically the compositional range from basalt to rhyolite in these drill cores (Leitch et al., 1988) matches that in the Boggabri Volcanics. This investigation also confirms recent views (Flood et al., 1988; Leitch et al., 1988; Leitch, 1993; Vickers, 1991, 1993) that Early Permian volcanic rocks differ from Late Carboniferous volcanic rock of similar silica content (cf Brownlow, 1982b; McPhie, 1984b).

A lack of identified regional marker units within the Early Permian volcanic pile prevents direct determination of the stratigraphic position of the Boggabri Volcanics. Thus it is still uncertain whether the Boggabri Volcanics correlate with the Warrigundi Igneous Complex (topmost volcanic rocks in the Werrie Basin) or with basal felsic volcanic rocks which underlie thick mafic volcanic rocks in AMOSEAS Quirindi No. 1 in the middle of the Gunnedah Basin (Russell, 1981) or with some other horizon. Therefore indiscriminate use of the term 'Boggabri Volcanics' for all felsic volcanic rocks in the Gunnedah Basin (Russell, 1981; Leitch and Skilbeck, 1991) is currently unjustified. Similarly the precise stratigraphic relationship between basalts at Boggabri (correlated with the Werrie Basalt by Hanlon, 1950) and those elsewhere in the Gunnedah Basin is unclear. These basalts are herein included in the Boggabri Volcanics as a matter of practicality.

The precise age of the Boggabri Volcanics is not yet known. No radiometric data are available. The only direct age dating known is a probable Stage 2 palynological age (Morgan, 1978) from varved shales in the Boggabri Volcanics. This sample was obtained by Brownlow (1981b) from drill core that penetrated the Boggabri Volcanics and overlying Leard and Maules Formation in the Leard State Forest near the eastern limit of Map 1. These varved shales are similar to the horizon correlated across the Namoi River and considered to be glacial in origin (McPhie, 1984b). Their possible Stage 2 age is consistent with poorly documented findings elsewhere in eastern Australia that glacial influence is stronger in Stage 2 then Stage 3a, for example, in the Galilee Basin (Evans, 1980). This data supports but does not prove, correlation with basal felsic volcanic rocks in the Gunnedah Basin rather than with the Warrigundi Igneous Complex.

## DEPOSITIONAL ENVIRONMENT AND PALAEOGEOGRAPHY

### Depositional Facies

Most mappable rock units are extensive, compositionally uniform, crudely tabular masses of coherent rock (some glassy) that lack vitroclastic textures, suggesting that they formed as terrestrial lava flows or domes (Cas and Wright, 1987; McPhie et al., 1993). Common presence of laminar flow banding, sparse occurrence of lithologically identical breccia with some, and occurrence of basal pitchstones with some are consistent with this interpretation. Formation of basal pitchstone, and of rare hyaloclastites is tentatively attributed to flow of lavas over wet ground. $SiO_2$ was added during formation of pitchstones, devitrification of overlying rhyolite, and formation of agate geodes, and CaO was added and alkalis leached during at least the first of these processes. CaO and $SiO_2$ were probably derived from groundwater which would probably have been alkaline due to alteration of silicates in the volcanic pile to chlorite, clay and carbonate (Loughnan, 1969).

Several white rhyolitic lavas around Gins Leap and Barbers Pinnacle are underlain by thin ignimbrites, which have been converted to pitchstone along with the bases of the overlying lava flows. These could have been rheomorphic ignimbrites (cf Cas and Wright, 1987, McPhie et al., 1993) that were welded densely and then flowed over wet ground. Interaction with wet ground prior to dense welding is unlikely as that could have prevented welding, and possibly given rise to a variety of water-contact features (Cas and Wright, 1987, McPhie et al., 1993). The recognition of these ignimbrites is further evidence that the overlying rock masses are lavas and not rheomorphic ignimbrites.

Coarse, polyvolcanic, lithic breccias with clasts up to 300 mm in diameter and enclosed within densely welded zones of some ignimbrites are interpreted as co-ignimbrite lags formed close to vent due to eruption column collapse (Cas and Wright, 1987).

## Volcanic Environment

Various features indicate that the Boggabri Volcanics are remnants of former eruptive centres or their immediate environs, including: possible plugs (e.g., Barbers Pinnacle) and other small intrusives; inferred calderas; the predominance of lavas including domes which are probably endogenous (Cas and Wright, 1987; McPhie et al., 1993); common vitrophyric and densely welded zones in ignimbrites; and co-ignimbrite lags (Cas and Wright, 1987; McPhie et al., 1993). Greater abundance of ignimbrite compared to lavas amongst rhyolites in the subsurface Gunnedah Basin (Leitch and Skilbeck, 1991; Leitch, 1993) supports this interpretation.

Sediments in the Boggabri Volcanics appear to be locally derived (all from Boggabri Volcanics-like lithologies). Slight elevation leading to erosion of poorly consolidated deposits is inferred from the conspicuous lack of thick air-fall tuffs, and rarity of sedimentary rocks (poor outcrop is probably also a partial explanation). Sporadic coarse-grained sediment is consistent with localised uplift associated with volcanism (e.g., caldera formation).

Further evidence for a terrestrial environment includes: common welding in ignimbrites; sparse plant fossils (McPhie, 1984b); and a lack of evidence for interaction between most rock masses and standing water (e.g., pillow lavas, explosion breccias, thick hyaloclastites). Lack of marine fossil, sedimentary indicators of marine deposition, or of sea-water alteration indicates a terrestrial environment. Sparse hyaloclastites, pitchstone bases to some lavas and ignimbrites and minor well-bedded sediments implies intermittent availability of fresh water. The presence of varved shales implies glacial conditions (McPhie, 1984b).

The presence of felsic flows that are generally thinner, and apparently more laterally continuous compared to those of classic calc-alkaline settings (cf. Cas and Wright, 1987) and a common tendency for ignimbrites to be welded, is consistent with the high temperature inferred from Fe-Ti oxides in many basaltic to dacitic rocks (see Mineralogy chapter), and with the lower intrinsic viscosity that would arise from a marginally sub-alkaline to mildly alkaline composition.

## Development Sequence

The interbedding of basalt and rhyolite in the Healthcliffe section and lower part of the Quarry section, and especially the occurrence of basalt underlying a sedimentary horizon (in both) (i.e. a local hiatus in major volcanic activity) suggest a possible evolutionary sequence: rhyolite ignimbrite (optionally), then rhyolite lava, then basalt followed by quiescence and sporadic sediment deposition.

## Facies Models and Regional Palaeogeography

Boggabri Volcanics most closely resemble those volcanic rocks that form in a continental silicic setting (Cas and Wright, 1987; see also McPhie, 1984a). They comprise clusters of rhyolite hills (lava domes and short flows) plus localised calderas and collapse breccias and minor caldera-fill sediments. However, an underlying ignimbrite shield (Cas and Wright, 1987) is not well developed, except perhaps in the Daisymede Domain.

A continental stratovolcano model is inappropriate due to a lack of prominent lahars, plinian air-fall deposits, scoria and fluvial deposits or erosive channelling, and therefore Boggabri Volcanics differ from the Werrie Volcanics near Wingen (Vickers 1991, 1993). A continental basaltic model (Cas and Wright, 1987) is also inappropriate due to a dominance of felsic rocks.

This model and the above data are broadly consistent with formation of the Boggabri Volcanics in a subsiding basin uninfluenced by the erosion of proximal mountains that characterised the Late Carboniferous (Brownlow, 1978; Flood et al., 1988).

A Stage 2 age (rather than a Stage 3b age) for the Boggabri Volcanics would imply that the Boggabri Ridge was elevated throughout the remainder of the basalt-dominated Early Permian volcanism (Leitch et al., 1988; Leitch 1993) because there is no evidence of erosion of a thick basalt pile (the only evidence for erosion of the Werrie Basalt is the extensive but thin flint-clay bearing Leard Formation — Loughnan, 1975; Brownlow, 1981b). However, elevation of the ridge was then probably slight because erosional products from the Boggabri Volcanics have not been recognised within the Werrie Basalt. Possible derivation of the Temi Formation underlying the Werrie Basalt in the western NEO (McPhie, 1984b) would be consistent with a Stage 2 age for the Boggabri Volcanics. The fine grained nature of the Goonbri Formation locally overlying the Boggabri Volcanics east of the Boggabri Ridge implies low relief during Stage 3b age (post-volcanic) sedimentation. Intense weathering of volcanic rocks (the inferred source of the Leard Formation) is also indicated at this time (Loughnan, 1975; Brownlow, 1981b).

## COMPOSITIONAL VARIATION

The Boggabri Volcanics comprise a range of compositions from basalt to rhyolite. Most select samples are altered, especially the rhyolite pitchstones. The latter have gained $SiO_2$ and CaO and lost alkalis, especially $Na_2O$, which probably accounts for their apparently peraluminous composition.

### Fractionation

The ubiquitous presence of plagioclase and oxides, orderly appearance or disappearance of phases and broad compatibility of phase assemblages suggests that fractionation was a major cause of the Boggabri Volcanics compositional range. Thus basalts are linked by a common troctolitic phenocryst assemblage (olivine-Cr spinel-plagioclase). Groundmass mineralogy in basalts (2 or three pyroxenes, plagioclase and Fe-Ti oxides) provide a link with andesites. Andesites and dacites are linked by gabbroic or dioritic phenocryst assemblages and the common presence of 2 or 3 pyroxenes, prominent Fe-Ti oxides and apatite and by the absence of quartz, amphibole (most rocks) and olivine (most rocks). Rhyolites are linked by a restricted plagioclase range, rarity of quartz, apparent absence of K-spar, restricted ferromagnesian assemblage and the typical presence of zircon. The incoming of zircon and the other changes are broadly consistent with fractionation. In addition, $SED_{05}$ and $SMPR_{06}$ are linked by similar phases as well as similar mineral and original glass chemistries. The MORB-like plagioclases (low Or) are consistent with fractionation producing strong K-enrichment.

### Main Trend as a Fractionation Trend

The (near) co-incidence of many data with the Main Trend (especially the Intermediate Segment — Appendix 2), justifies its use as a frame of reference in reconnaissance assessment of comparative diagrams as well as its consideration as an evolutionary trend. Two well developed inflections (e.g., on **$TiO_2$ v Zr**) strongly indicates crystal fractionation as a major source of variation among Boggabri Volcanics. Moreover, the Main Trend is broadly compatible with the orderly appearance and disappearance of phases cited above, for example, troctolitic fractionation is broadly compatible with the Mafic Segment.

The Main Trend has many currently unavoidable limitations: (a) use of reconnaissance standard INAA for some elements; (b) use of imprecise XRF data for some elements near detection limit; and (c) use of rocks that are altered such as pitchstones, or have been adversely affected by eruptive processes (e.g., ignimbrites). Further there are too few data to: (a) use appropriate logarithmic curves (followed by fractionation trends — Rollinson, 1993), rather than linear trends are used herein, (b) establish critical trend points statistically; and (c) differentiate data points that are on adjacent but discrete trends. These limitations probably account for problems such as unreal negative values for Ni at the Mafic Inflection and for Cu and MgO at the Felsic inflection, as well for low P at the calculated Mafic Inflection leading to an Intermediate Segment that mimics data poorly. Similarly, $SPB_{39}$ was probably not derived directly from $SOB_{12}$, because troctolite fractionation would produce a slightly flatter trends. The Felsic Trend is especially problematic because it was defined using a select rhyolite with low HFSE ($SLPR_{08}$), but would not be greatly changed by substituting the only available biotite rhyolite lava ($SFBR_{04}$). Finally, defining a 'liquid line of descent' requires use of glasses or aphanitic rocks, whereas Boggabri Volcanics are typically porphyritic (Cox et al., 1979).

Despite needing refinement, the Main Trend with two inflections and three contiguous segments is probably valid in concept and hence correctly indicates the importance of fractionation as a mechanism in producing the compositional diversity of the Boggabri Volcanics. This implies that one narrow mafic source range is needed for many of the Boggabri Volcanics.

## Other Causes of Variation

Several samples are anomalous:

a. $SOA_{10}$ contains a hybrid assemblage of olivine (basaltic affinity) and evolved augite plus coarse apatite (dacitic affinity). It consistently plots off the Main Trend, close to Cross Trend 2 for some element, suggesting mixing of basalt and evolved dacite.

b. Two leucocratic pyroxene rhyolites ($SLPR_{29}$ and $SLPR_{08}$) contain slightly lower HFSE compared to leucocratic biotite rhyolites (Appendix 2), suggesting separate sources. Fractionation to lower HFSE is possible, but unlikely to produce a relatively dry melt (pyroxene rhyolite) from a wetter one (biotite rhyolite), unless the water were externally derived, in which case addition of F would be required to match that in the biotites (i.e. a very complex scenario).

c. $SAD_{24}$ (vitrophyre forming a dyke) also contains lower HFSE compare with Main Trend equivalents (e.g., on **$TiO_2$ v Zr**). Fractionation along the Dyke Trend or nearby is unlikely, because ilmenite would have to cease precipitation, yet is present in all rhyolites. A low HFSE source is indicated.

d. Abundant, coarse zircon and high Zr in #40 (leached dacite?) is anomalous and could be due to crystal enrichment in zircon during fractionation and/or derivation from a high HFSE source.

e. Two rhyolitic ignimbrites ($SLPR_{13}$ and $SFBR_{25}$) have petrographic and trace element evidence (e.g., sparse basaltic lithics and anomalously high Ni) that implies basalt contamination, probably during eruption; loss of glass to ash clouds could also have slightly depleted the rock in incompatible elements.

Thus $SLPR_{29}$, $SLPR_{08}$ and $SAD_{24}$, probably require a separate low HFSE source, #40 might need a separate high HFSE source, but $SOA_{10}$ and the ignimbrites probably differ only through magma mixing or eruptive processes respectively. A separate high HFSE source for #40 might resemble that required for the unassigned volcanics.

## A Test of Magma Mixing

Magma mixing can be tested. $SOA_{10}$ contains intermediate Cr and intermediate $SiO_2$ (62 ppm Cr and 58.28% $SiO_2$, anhydrous basis). Select basalts that define the Mafic Segment are characterised by low $SiO_2$ (≈ 50%) over a range of Cr values (245 ppm for $SOB_{12}$, 123 ppm for $SPB_{39}$). In contrast the Intermediate Segment and associated select Boggabri Volcanics are characterised by low Cr (<18 ppm) at andesitic and dacitic $SiO_2$ values. These latter two compositional ranges are consistent with fractionation of an element with a high bulk partition co-efficient.

Producing $SOA_{10}$ by fractionation would presumably require a source with basaltic $SiO_2$ values but peridotitic Cr values (≈ 2500 ppm) or higher because of the high bulk partition co-efficient of Cr. Such a source is unlikely, as is an origin by fractionation (reinforcing a magma mixing interpretation). It should be noted that this argument would appear to be generally applicable, and indicates mixing of basaltic (high-Cr) and felsic (low-Cr) components to explain the intermediate Cr at intermediate $SiO_2$ in Average Continental Crust and many of the mesocratic granitoids used herein for comparison (see Figs A2.2–A2.30 in Appendix 2).

# MAGMATIC SOURCE

## Compositional Affinity

The Boggabri Volcanics are of subalkaline to mildly alkaline affinity and display an unusual combination of features: basalt petrology, plagioclase chemistry, high Zr/Nb and other ratios typical of primitive MORB, high $Al_2O_3$ and MORB-normalised Ba, Pb and Sr and low MORB-normalised Nb typical of arcs, a Zr-Hf-Sm anomaly and other features indicating a source like Hawaiian Nepheline Melilitite. Other features (depleted HREE and high Mg/Cr, high Ni/Cr, high Cs and low Hf, and intermediate MORB-normalised K, Rb and Pb) are typical of these settings. Thus their compositional affinity is equivocal and may not have been described previously (Vickers, 1993) because discriminant analysis, petrogenetically significant ratios and REE analysis (Appendix 3), elemental abundance plots (Appendix 2), elemental abundance spectra (see Geochemistry chapter), and comparative bivariate plots (Appendix 2), yield contradictory results, variously indicating or negating all common melt environments depending on the parameters used.

## A Single Source

No single, common geochemical reservoir or reference composition is an adequate source for $SOB_{12}$. All but Hawaiian Nepheline Melilitite lack the Zr-Hf-Sm anomaly. Primitive MORB and E-MORB are too low in LILE, whereas OIB and Hawaiian Nepheline Melilitite and too high in them, and all lack an arc signature. Continental comparators (Appendix 2) are too high in Si and LILE (except Pb) and too low in Mg-Cr-Ni, although Average Continental Crust provides an approximate match in the middle of the incompatibility spectrum and the Mole Granite LILE signature (apart from Pb) approximates the composition of the component removed to produce the $SOB_{12}$ arc-like signature. Fuji basalt (an indicative arc basalt) has a broadly similar element abundance spectrum but is systematically enriched in HREEs and LILE, and depleted in Mg-Cr-Ni. Rindjani basalt was specifically chosen from a database of primitive arc basalts (Appendix 2) because it was the only one that matched $SOB_{12}$ in Si, Cr, Al, and P (a difficult combination for other sources). It also matches Fe, Eu, Na, and Ce reasonably well, but is depleted in Mg, Ni and Sr, and enriched in Nb, LILE (except Sr), Hf and HREE.

## Mixing Models

A simple mixing model is also negated by complementary relationships (Appendix 2). MORB is the most widely available basaltic melt, so is an obvious candidate as the major component in any mixed melt. However, no other single component can provide the arc signature, Zr-Hf-Sm anomaly and HREE depletion which are all needed to complement MORB. Arc basalts could provide an arc signature, and tholeiitic or boninitic melts could provide HREE depletion but lack a Zr-Hf-Sm anomaly. Rindjani basalt provides the best match among available primitive arc data, but is too enriched in most LILE and HREE, and also highly atypical of arc rocks. Besides, arc basalts are of mixed origin and therefore primary sources should be sought (Arculus, 1994). This leaves a further problem: OIB and Hawaiian Nepheline Melilitite are the only non-arc sources that can complement Primitive MORB as a source of P, but none can provide the high Al (see Appendix 2). Whether this reflects plagioclase accumulation (Crawford et al., 1987; Kersting and Arculus, 1994) or an Al-enriched source (Pearce et al., 1992) is unclear.

Thus a mixing model would need to consider at least three components: a MORB-like component, but even more depleted (or involving unusually high degrees of partial melting); an arc component (from fluids or as pelagic sediment — Hole et al., 1984; Weaver, 1991; Pearce and Parkinson 1993; Arculus, 1994) that is depleted in some LILE (generally those other than Pb that are elevated in Mole Granite); and a source of P and a Zr-Hf-Sm anomaly. The latter source would probably be a Hawaiian Nepheline Melilitite or a similar melt. Low Cr also need to be accounted for. Further, the flat HREE pattern requires the whole process to occur without leaving residual garnet (Thirwall at al., 1994) unless positive and negative slopes among different components counterbalance.

## Source Modelling

Pearce and Parkinson (1993) modelled mantle sources by normalising elements that are not part of the 'arc signature' (Fig. 30a) to Fertile MORB Mantle (FMM). For consistency, Ca is plotted to the left of Al as on their diagrams, but note that their theoretical models generally have Ca>Al, whereas their modern examples more commonly have Ca<Al. Also their FMM estimate is broadly similar to pyrolite (McDonough and Sun, 1995) except for low Nb (≈0.3x pyrolite).

$SOB_{12}$ normalised to FMM (Fig. 30a) displays VHI>>HI≈MI (very highly, highly and moderately incompatible elements) with Nb at 20.5x FMM, a virtually straight line trend for Nb-Zr-Ti-Y (range 20.5x to 3.9x FMM), Y=Yb=Ca+Al (≈4x FMM), and a steady decline from Al to Mn=Fe except for a slight peak at V, then a steep drop through Mg to Cr ≈ Ni (0.09x FMM). This pattern differs from theoretical models in the strikingly low Cr and the lack of discrete steps at the boundaries of VHI, HI, MI and SI/SC (slightly incompatible/slightly compatible) elements, and does not match any figures in Pearce and Parkinson (1993). $SOB_{12}$ is probably closest to Scotia Sea overall, but lacks the distinct Ca anomaly, is closest to Grenada (Shimizu and Arculus, 1975) for more incompatible elements except for low Ca in the latter, and is closest to Eifuku (Marianas)

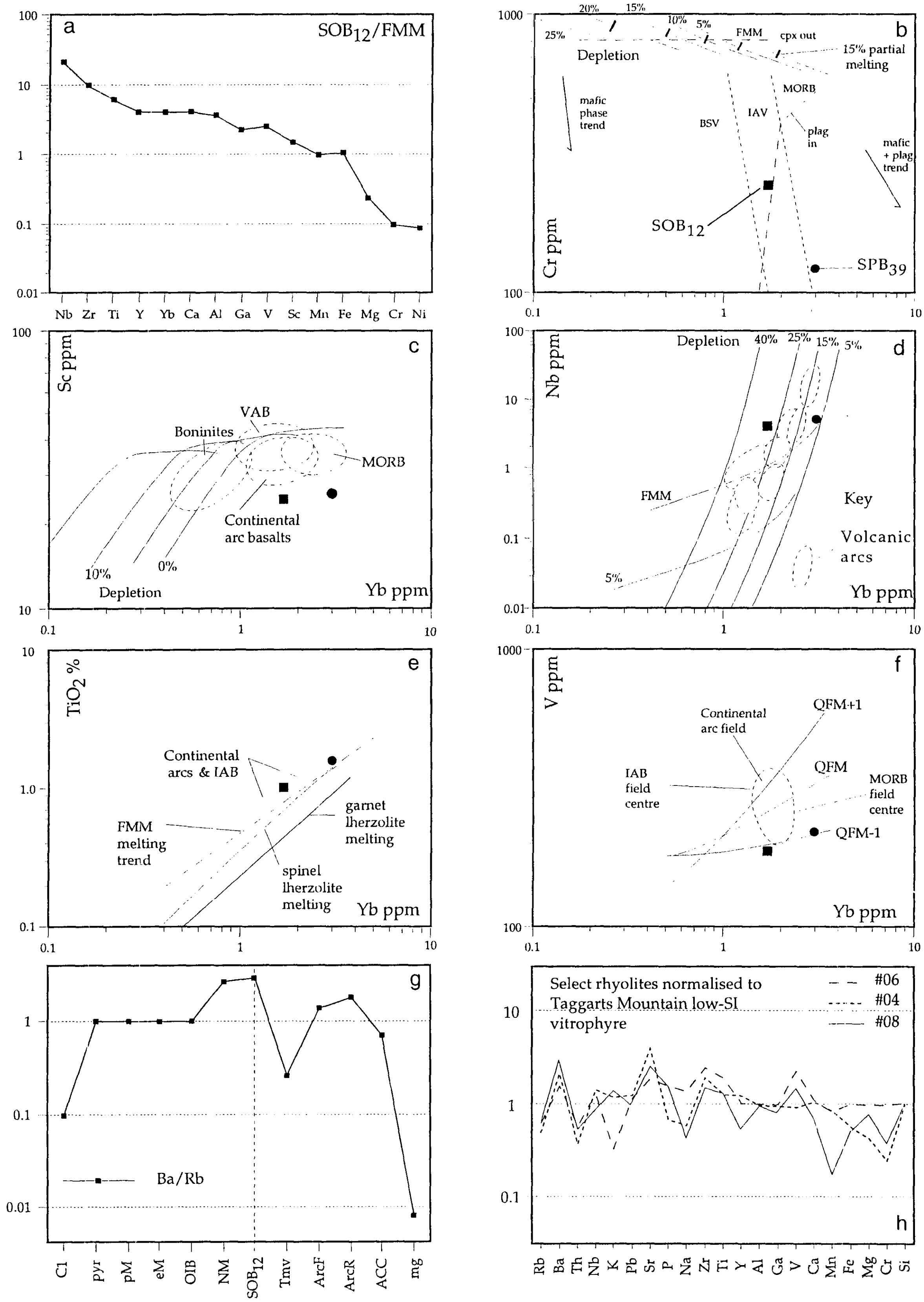


**Fig. 30** Source modelling. (a) SOB12 normalised to FMM. (b–f) Cr, Sc, Nb, $TiO_2$ and V in SOB12 (solid square) and SPB39 (solid circle) plotted against Yb (after Pearce and Parkinson, 1993). (g) Normalised Ba/Rb in SOB12 (solid squares). (h) Several select rhyolites normalised to average low-Si rhyolite vitrophyre from Taggarts Mountain Ignimbrite Member (McPhie, 1984a).

in pattern shape for SI-HC (highly compatible) elements but at slightly lower values.

The lack of a simple fit suggests the need for a more complex model, probably involving mantle enrichment to match Nb, depleted mantle to match Y and Yb, and possible a non-arc component to match low V and Sc. Melting leaving residual garnet would model the low Sc, but is denied by Y=Yb in $SOB_{12}$, unless superimposed on a depleted source (Ti≤Y<Yb). Low Cr could be due to melting of spinel lherzolite at $1200^{o}C$ (higher partition coefficient at lower temperature), or to prior depletion through melting of hornblende lherzolite at $1300^{o}C$ (Fig. 4 in Pearce and Parkinson, 1993). The latter process would retain Ti and could therefore explain the high Ti/Y. Further modelling is required to resolve these discrepancies.

Fig. 30b–f (Pearce and Parkinson, 1993) provide additional constraints. **Cr v Yb** (Fig. 30b) indicates that $SOB_{12}$ plots in the IAV/ Continental arc field, anomalously just above the plagioclase-in line and could be produced by about 25% partial melting of FMM or 1–2% melting of 10% depleted FMM (or an intermediate combination). The former is supported by the lack of phenocrystic augite in $SOB_{12}$ which suggests possible elimination of clinopyroxene (requiring about 25% cumulative melting) from the source. **Sc v Yb** (Fig. 30c) indicates that Boggabri Volcanics are highly anomalous and plot below all major fields. **Nb v Yb** (Fig. 30d) indicates that $SOB_{12}$ is anomalous compared to representative arc fields, and would require about 30% partial melting of FMM enriched about 3% in VHI elements. **$TiO_2$ v Yb** (Fig. 30e) shows that $SOB_{12}$ plots in the arc basalt fields and would require a spinel lherzolite, rather than garnet lherzolite, source. **V v Yb** (Fig. 30f) shows that $SOB_{12}$ plots outside arc and MORB fields but is offset from the centre of the MORB field parallel to the QFM+1 trend. That is, $SOB_{12}$ could have formed under MORB conditions from a source that had previously been depleted under arc conditions.

## A Proposed Model

A possible explanation of these contradictory data (subject to refinement and testing) is that FMM was (a) enriched in a subduction zone, imposing an arc signature; (b) then depleted in an arc environment under hornblende lherzolite conditions leaving both a DMM signature (including depleted VHI and HI elements, depleted Cr and V, slightly depleted Sc and high Ti/Y) and a residual arc signature preferentially depleted in alkalis and Th relative to alkaline earths and Pb; and (c) was then mobilised and enriched ('mantle metasomatised') by a small volume melt derived from depth (garnet in residue) that reversed the depletion in HI elements, enriched VHI elements, exacerbated the low residual Sc and promoted low temperature melting (about $1200^{o}C$). Such a melt could have been a nephelinite or carbonatite (McDonough and Sun, 1995; Yaxley et al., 1991).

Effectively, the Boggabri Volcanics source would have been doubly depleted and doubly enriched.

The arc component lost to produce the residual arc signature (Fig. 30g) probably has a similar MORB-normalised signature to the Mole Granite apart from low Pb, which suggests that Boggabri Volcanics magmas interacted very little if at all with continental crust during their ascent and emplacement. (Mole Granite is highly fractionated — Chappell and Bryant, 1994; loss of a granitic component similar to a minimum melt composition might suffice).

Minor variations in the proportion of nephelinite could produce both a low HFSE source (probably appropriate for $SAD_{24}$, $SLPR_{29}$, and $SLPR_{08}$), and a high HFSE source (possibly appropriate for #40 and the unassigned volcanics). The latter comment suggests that the unassigned volcanics are part of the Boggabri Volcanics despite equivocal field relationships.

### Regional Affinity

Regional petrochemical affinity is important because the melt environment could not be established from literature data, and hence must be deduced from its regional context. Regional affinity is only established for the Werrie Basalt (Vickers, 1991, 1993) but is likely for the remaining volcanic rocks of the SBB and western NEO, based on limited published data (see Geochemistry chapter). Boggabri Volcanics differ from Late Carboniferous volcanic rocks of the western NEO, and all intrusive suites and all Early Permian volcanic rocks of the central and eastern NEO (Appendix 2). Elemental abundance plots of select Boggabri Volcanics rhyolites normalised to low-Si rhyolite vitrophyre from the Late Carboniferous Taggarts Mountain Ignimbrite Member (McPhie, 1984b) demonstrated both broad similarity and a distinctive residual arc signature in the Boggabri Volcanics (relatively high Ba, low Rb — Fig. 30h).

Thus, Boggabri Volcanics could be indicative of a major petrographic province encompassing the SBB and adjacent margins of the LFB, TFB and NEO, and possibly extending into North Queensland (cf McKenzie, 1987). However, that province is distinct from igneous activity in the central and eastern NEO which would comprise a separate province (or provinces).

## REGIONAL GEOLOGICAL SETTING

### Overview

Recent models for the development of the NEO and adjacent SBB during the Late

Carboniferous, Permian and Triassic variously envisage:

- A Late Carboniferous Andean-type continental margin, comprising an arc in the vicinity of the Sydney and Gunnedah Basins, a fore arc represented by the parts of the Tamworth Belt and Hastings Block of the NEO, and an accretionary complex represented by most of the rest of the NEO (e.g., Harrington and Korsch, 1985; Murray et al., 1987; Scheibner, 1989; various papers in Flood and Aitchison, 1993).
- A change to an extensional regime in the Early Permian, resulting in widespread basin formation (including the SBB). and rift-related? volcanism possibly related to a transtensional regime (e.g., Carey, 1969; Cuddy, 1978; Degeling and Runnegar, 1979; Cawood, 1982; Korsch, 1982; Flood et al., 1988; Scheibner, 1989; Korsch et al., 1993; Leitch, 1993; see also Table 8 and Appendix 5).
- Deformation and igneous activity in the central NEO during the transition (or hiatus) between the above two regimes (Shaw and Flood, 1981; Korsch, 1982; Murray et al., 1987; Roberts et al., 1991, Collins et al., 1993; see also Appendix 5).
- Sedimentation in the SBB during a thermal relaxation or 'sag' phase following volcanism contemporary with multiple Permo-Triassic tectonic and thermal regimes in the NEO as well as intermittent uplift in the LFB, shedding detritus into the SBB and other basins (Brownlow, 1981a, 1988b; Veevers et al., 1993; Scheibner, 1993; Tadros, 1993b; see also Appendix 5).

Table 8 summarises numerous models for the origin of the Sydney Basin (Scheibner, 1993, modified from Murray, 1990). Only those that specifically discuss the volcanism are considered herein; other proposals are more relevant to the subsequent history of the SBB (see Appendix 5).

## Igneous Activity and Sedimentation

Early Permian igneous activity and sedimentation are manifest as three broad zones:

- The SBB and immediate environment comprising thick, laterally continuous, volcanic-dominant sequences (e.g., Boggabri Volcanics). This zone overlaps the presumed Late Carboniferous arc in New South Wales and possibly North Queensland suggesting continued development of, or reactivation of, that zone (Flood et al., 1988; Brownlow, 1988b, Appendix 5).
- An eastern zone in central and eastern NEO of thick marine sedimentary sequences with localised development of volcanic rocks, and also including uplifted areas of Carboniferous S-type granitoids and metamorphic complexes and Early Permian S-type granitoids and mafic complexes (e.g., Brownlow 1982b; Cawood, 1982; Korsch, 1982; Shaw and Flood, 1981; Hensel et a., 1982, 1985; see also Appendix 5).

**Table 8: Previous Models for the Origin of the Sydney-Bowen Basin**

| *Basin-forming Mechanism* | *Tectonic Model* | *Process* | *References* |
|---|---|---|---|
| 1. Thermal | (a) Mantle diapirs | Rifting, volcanism and thermal subsidence following emplacement of mantle diapirs into the crust. | Brownlow 1981a; 1982a, b; 1988a, b, c |
| | (b) Thermal collapse | Cooling of crust/mantle after initial thinning. | Murray 1990 and others |
| | (a) Rifting | (i) Formation of a tensional volcanic rift between the Lachlan and New England Fold Belts (Gunnedah and Sydney Basins), transitional to a volcanic arc in the north (Bowen Basin) | Scheibner 1974a; 1976; Murray 1990 |
| | | (ii) Precursor rift to Mesozoic breakup, failed arm (?aulacogen) model | Harrington 1982; 1984 |
| | (b) Back-arc extension | Unspecified back-arc extension adjacent to a calc-alkaline volcanic arc (Bowen Basin) | Fielding 1990 |
| | (c) Back-arc spreading | Subsidence of craton behind eastward-migrating island arc system (Bowen Basin) | Battersby 1981 |
| 2. Thinning | (d) Extensional (simple shear) | (i) Formation of west-tilted half grabens by rotation of fault blocks along steep east-dipping faults (Denison Trough) | Paten, Brown & Groves 1979; Brown, Elliott & Mollah 1983; Ziolkowski & Taylor 1985 |
| | | (ii) Extension on shallow east-dipping major mid-crustal detachment fault, with north-east trending transfer faults (Bowen Basin) | Hammond 1987; Hammond & Mallett 1988; Mallett, Hammond, Leach, Enever & Mengel 1988a; Mallett, Hammond & Sullivan 1988b |

**Table 8: Previous Models for the Origin of the Sydney-Bowen Basin (Cont.)**

| *Basin-forming Mechanism* | *Tectonic Model* | *Process* | *References* |
|---|---|---|---|
| | (e) Transtensional | Extension accompanying strike-slip motion along Burunga-Goondiwindi-Mooki Fault System | Korsch, Harrington, Wake-Dyster, O'Brien & Finlayson 1988; Korsch, Wake-Dyster & Johnstone 1990 |
| | (f) Strike-slip (pull apart) | (i) Graben formation due to north-west-oriented dextral rotational force couple | Evans & Roberts 1980 |
| | | (ii) Large-scale strike-slip motion along Burunga-Goondiwindi-Mooki Fault System (transform fault) | Harrington & Korsch 1979; 1985; Harrington 1982; 1987 |
| 3. Load | (a) Retro-arc foreland basin | Subsidence due to load of volcanic arc along eastern margin (Bowen Basin) | Murray 1985; Fielding 1990; Fielding, Falkner, Kassan & Drapper 1990 |
| | (b) Fold - thrust belt foreland basin | Subsidence due to sediment supply from and load of west-directed fold - thrust belt along eastern margin (from Late Permian) | Scheibner 1976; Jones, Conaghan, McDonnel, Flood & Shaw 1984 |
| | (c) Fore-arc trough | Subsidence adjacent to volcanic arc - mountain belt | Jones & McDonnell 1981; Conaghan, Jones, McDonnel & Royce 1981 |

*Source:* Scheibner (1993), after Murray (1990) (see original papers for references).

Note: the model actually presented by Brownlow (1981a) involved mantle intrusion to the crust-mantle boundary, causing crustal melting in the Late Carboniferous, basaltic intrusion associated with 'embryonic sea floor spreading' in the Early Permian, and subsequent subsidence during cooling analogous to that modelled by Falvey (1974) for Atlantic-type margins. The importance of the thermal history in the origin of the basin and of multiple thermal and deformational processes in the subsequent history of the region was first proposed by Brownlow (1977a), although the brief published abstract only mentions a 'theoretical tectonic model'.

- A western zone in the LFB of thick sedimentary sequences apparently devoid of volcanic rocks (e.g., Scheibner, 1989).

## Structural Setting

**NNW trending basins**, broadly parallel to the regional structural grain are prominent in the above three zones (Fig. 31, see also Appendix 5). These basins include the Ovens Graben in south-western New South Wales, the **Gunnedah and Bowen Basin** segments of the SBB, and many basins in the NEO (e.g., Evans and Roberts, 1980; Korsch and Harrington, 1985; Scheibner, 1989; Leitch, 1993; Sliwa et al., 1993). A systematic offset along a major, NE-trending, right-lateral dislocation that crosses the SBB close to Queensland-New South Wales border means that Bowen Basin is along strike from basins in the eastern part of the southern NEO (especially parts of the Texas Block and the Dyamberin Block). Syndepositional faulting is recognised in many of these basins especially associated with Stage 2 sedimentation (e.g., half grabens in the Denison Trough — Korsch et al., 1993).

**NS trending basins** are also prominent in the Early Permian geology of eastern Australia, and include (from W to E): the **Taroom Trough and the Sydney Basin segments of the SBB**, the Gloucester Basin in the southern Tamworth Belt, and basins along the western margin of the Hastings Block in the NEO (e.g., Evans and Roberts, 1980; Korsch and Harrington, 1985; Scheibner, 1989; Leitch, 1993; Sliwa et al., 1993). In addition, NS trending faults divide the southern Tamworth Belt into the Rouchel, Gresford and Myall Blocks (Roberts et al., 1991), and the western margin of the Hastings Block trends northerly.

## Discussion

A simple cause of Early Permian volcanism by extension alone is negated by the far wider extent of extension than volcanism, by the apparent presence of two contrasting Early Permian volcanic belts (cf. Brownlow 1982b), and by the sparsity of volcanic rocks in some marine Early Permian extensional basins in NEO that have apparently suffered greatest extension.

The many models advocating arc volcanism (see Table 8) are negated by the recognition herein of a residual arc signature and MORB-like basalt petrology (assuming the Boggabri Volcanics to be regionally indicative). In addition, the SBB is 200–300 km inland and that is probably excessive for applying an arc model to both volcanic zones, especially as any subduction complex would have to be even further east. Even an arc producing potassic volcanic rocks from the breakdown of phlogopite (cf Tatsumi and

Eggins, 1995) would probably not be so far from its trench. Moreover, calc-alkalinity or an arc signature do not necessarily indicate contemporary subduction and arc volcanism. For example, the San Francisco Volcanic Field in the western USA contains abundant andesites and associated basalts, dacites and rhyolites that erupted at least 10 My after the cessation of subduction (Arculus and Gust, 1995).

Some models advocating rifting are apparently based on the historic assumption that the Early Permian volcanic rocks are bimodal and of alkaline affinity. However, Leitch et al. (1988) showed that the Early Permian volcanic rocks are not bimodal, and the Boggabri Volcanics alkaline tendency is only mild and does not mask sub-alkaline petrology.

Despite criticism by Scheibner (1993), one of the few models for the origin of the SBB (see also back-arc basin models in Table 8) that is consistent with MORB-like Boggabri Volcanics basalt petrology is the suggested 'embryonic sea-floor spreading' (Brownlow, 1981b). That suggestion was intended to convey a sense of pervasive, but mild and not necessarily well-organised, crustal extension possibly associated with basalt dyke injection in a broadly back-arc setting (indicative of the early stages of sea-floor spreading — cf Saunders and Tarney, 1991). Early cessation of such a process (hence 'embryonic stage') would have resulted in only limited transgression regionally, and no new oceanic crust or strong extension/detachment structures. Moreover, volcanic geochemistry at that stage of sea-floor spreading can involve a complex and unpredictable mixtures of MORB ± arc ± continental ± mantle metasomatic influences (Saunders and Tarney, 1991), broadly analogous to that inferred for the Boggabri Volcanics.

Early Permian extension is too widely developed to have occurred only in response to processes that originate in the two volcanic zones (cf Brownlow, 1988b), and therefore operation of an independent continental-scale stress-field is indicated. Basin formation along NNW trends would be consistent with pure extension due to NNW-SSE compression (cf Moody and Hill, 1956; Spencer, 1969; Evans and Roberts, 1980 — see Fig. 31). Such a stress field could also have produced ENE trending folds in the metamorphic complexes in central NEO (Farrell, 1988; Moody et al., 1993; Dirks et al., 1992) as compressional folds, NS trending faults in the southern NEO (as shear faults) and left-lateral drag folds in the southern NEO (due to regional simple shear Cuddy, 1978; Cawood, 1982; see also Appendix 5). These different mechanical responses were not necessarily synchronous, but could represent a progressive response as the Carboniferous subduction complex matured thermally and became work-hardened. Displacement of the Hastings Block from the southern end of the Tamworth Belt as well as faulting in the southern Tamworth Belts (Roberts et al., 1991, 1993) could have

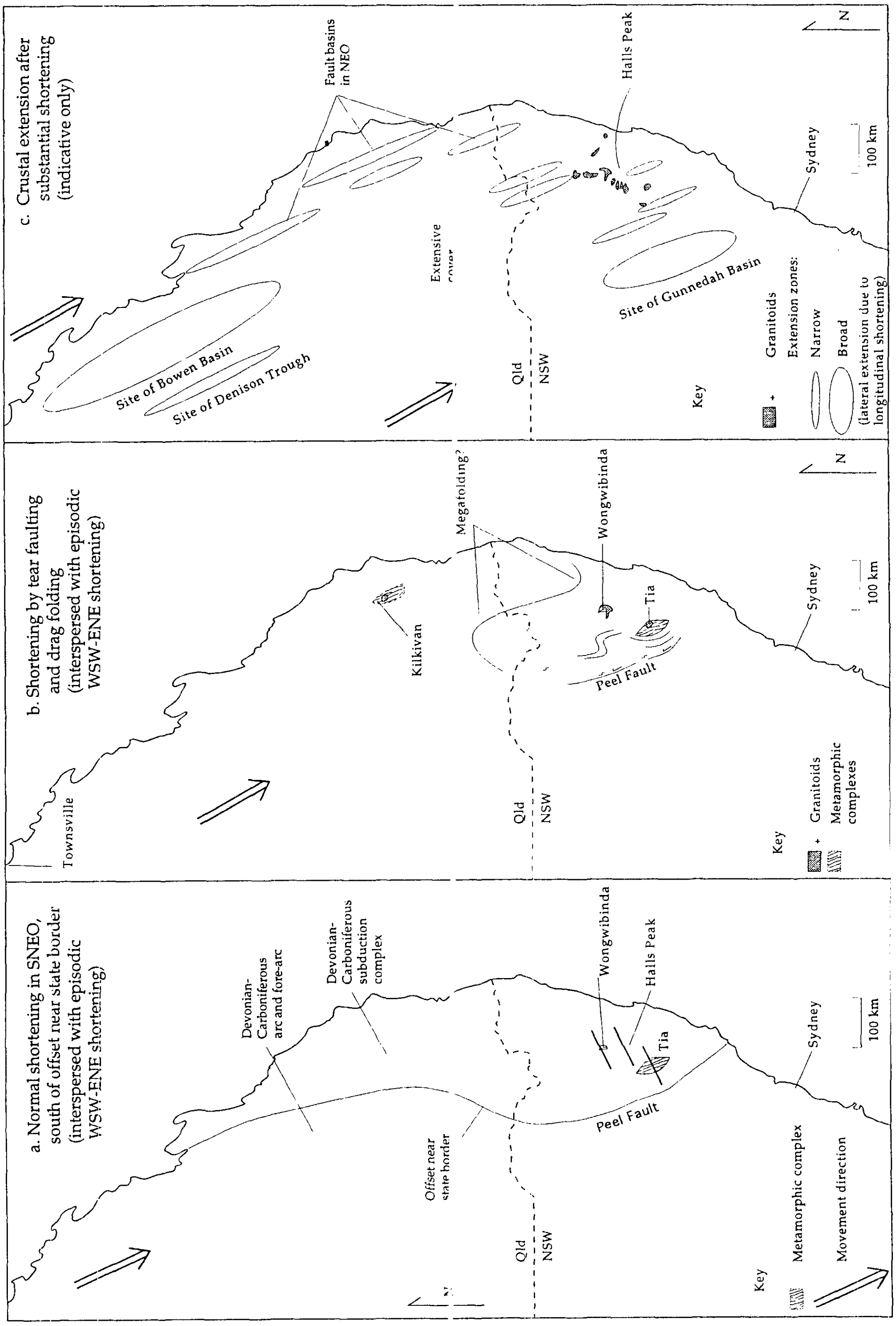


**Fig. 31** A model for the Permo-Carboniferous development of eastern Australia (see Appendix 5 for palaeogeographic details).

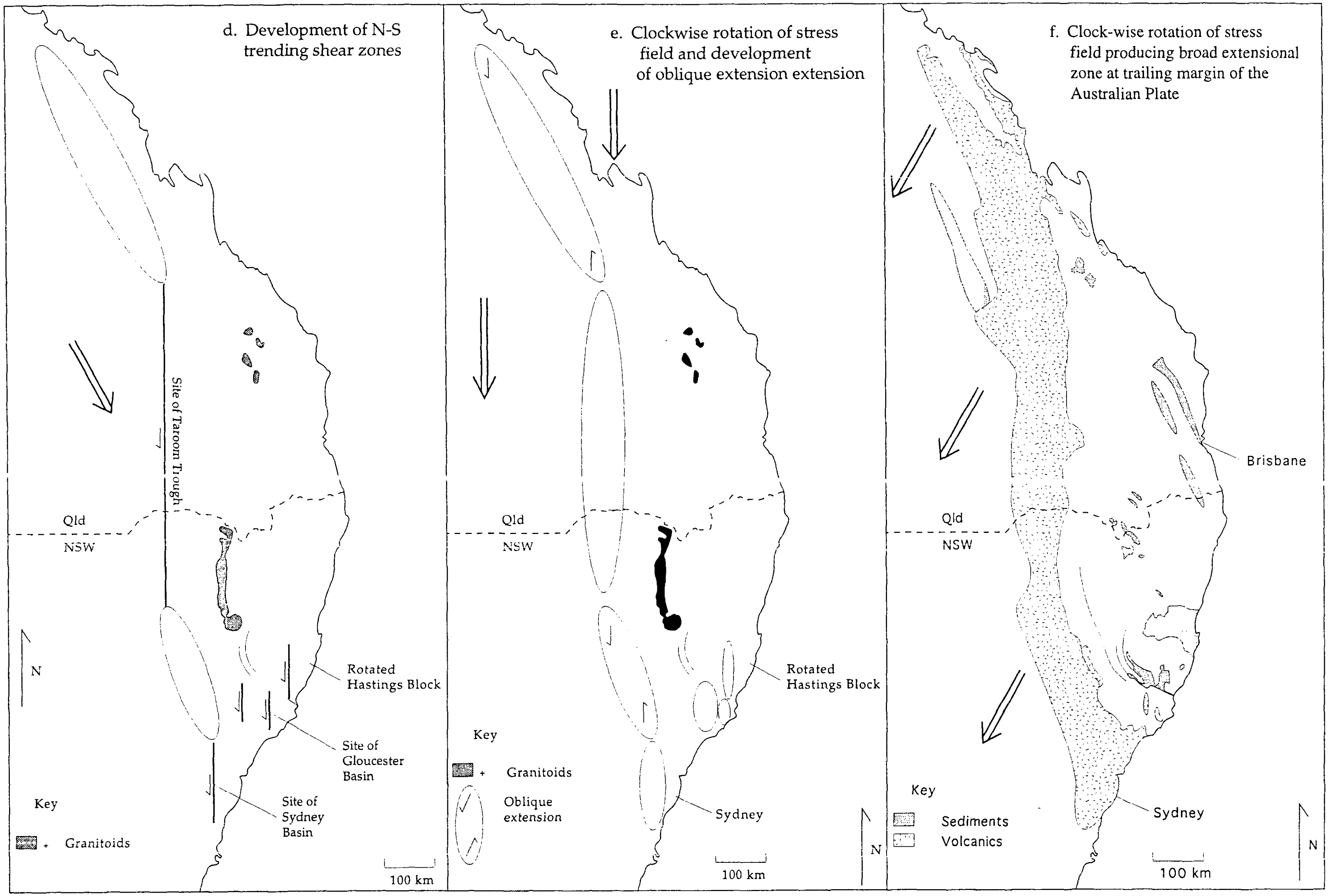


**Fig. 31** A model for the Permo-Carboniferous development of eastern Australia (cont.).

followed.

Extension in NS trending basin segments would be consistent with a more northerly directed compression leading to E-W pure extension. Both NNW-SSE and N-S trending compression could have developed sequentially through about a $20^{o}$ clockwise rotation of the stress field.

The major NE trending offset between Queensland and New South Wales geology would have been be a major factor because it would have juxtaposed the relatively weak subduction complex of the southern NEO along the principal stress axis (NNW-SSE or N-S) from the stronger continental hinterland of the northern NEO. Those contrasts could have concentrated shortening in the SNEO in a left-lateral shear regime, possibly causing megafolding (Murray et al., 1987), and enhancing development of oblique shear systems, whereas elsewhere, a simple shear regime might have dominated (see Appendix 5).

## A Model

These effects could all be accounted for by broadly southerly movement of the Palaeo-Australian plate, progressively causing (Fig. 31):

1. protracted SSE movement in the latest Carboniferous accommodated by compressive folding of the Carboniferous subduction complex;
2. drag along NNW-trending sutures, formation of drag structures, and possible megafolding in the subduction complex (possibly all contemporary with 1);
3. initiation of crustal extension in both the former subduction zone and adjacent continental margin as the former subduction zone strengthened;
4. left lateral shear movement along NS trending faults and enhanced extension in NNW trending structures (induced simple shear regime);
5. progressive clockwise rotation in the Palaeo-Australian enhancing southward plate movement relative to the continental margin (or northward movement of the Hasting Block and other parts of the continental margin relative to the continent), but would change the NS trend from a transpressional to pure extensional, and the NNW trend to oblique extensional; and
6. still further clockwise rotation in plate motion would change the whole continental margin to extensional as the Palaeo-Australian plate retreated from its former compressional zone.

The NNW trending compressional folds and foliation are prominent features of the Tia and Wongwibinda metamorphic complexes and require a further process to have operated during 1 and 2 above: continental margin-normal shortening during the latest Carboniferous. WSW-directed normal subduction of a mid ocean ridge to produce the

Permo-Carboniferous igneous activity in the eastern volcanic zone (Hensel et al., 1982) is a possible explanation. The exact correlation of igneous activity with the above sequence of events is unclear. Activity probably began in the metamorphic complexes late in the interval of NNW-SSE shortening of the subduction zone (1 and/or 2 above), and was possibly followed by intrusion of most Hillgrove granitoids during 3, Bundarra Plutonic Suite granitoids during 4 and/or 5, and Early Permian mafic complexes during 3, 4 or 5. Volcanism in this eastern zone would have occurred no earlier than 3, and possibly as late as 6. Mafic volcanism in the western volcanism was probably prominent during 6, but could have started earlier, and basal felsic volcanism could have occurred as early as 3.

Curved, broadly southerly movement of the Palaeo-Australian Plate in concert with brief westerly convergence of the Palaeo-Pacific Plate is an indicative rather than necessarily unique cause of the above stress field changes, and needs verifying using palaeomagnetics and other data. One test is provided by the shape of the Bundarra Plutonic Suite in the southern NEO. Its round a round 'head' in the south and a narrower, 200 km long 'tail' in the north and is reminiscent of the trace of a plume on a moving plate (P.G. Flood, pers. comm., 1993; cf Campbell and Griffiths, 1990); the boomerang shape of its tail is consistent with the plate motions suggested above.

Such a plate motion scenario could conceivably have created the conditions for reactivating the presumably still hot mantle-melt zone beneath the Late Carboniferous volcanic arc (Flood, et al., 1988; Brownlow, 1988b) through the addition of a small amount of nephelinite in an extensional setting. Whether the extensional regime mobilised the nephelinite and subsequently the Early Permian magmas, or merely facilitated their ascent is unclear and requires more detailed modelling in concert with a reexamination of the origin of the eastern volcanic zone.

Alternatives to the above abound, but space only permits consideration of three here. Firstly, traditional interpretations have implied a fixed continent, but that would necessitate especially complex movement of the Palaeo-Pacific Plate. Secondly, Collins et al. (1993) suggested that much of the complex deformation of the subduction complex occurred in the Late Permian, but that is probably mechanically unrealistic owing to the strengthening of the subduction complex that would have accompanied the Permo-Carboniferous deformation and igneous activity. Thirdly, Murray et al. (1989) indicated a gap in the Late Carboniferous volcanic arc between northern New South Wales and north Queensland; whether or not that gap is valid and poses a problem for this model remains to be determined.

# Chapter 7: Conclusions

This investigation has examined the composition, development and geological setting of the Boggabri Volcanics. In doing so, it has established that the Boggabri Volcanics:

- comprise basalts, andesites, dacites, pyroxene rhyolites and biotite rhyolites, mainly manifest as lava flows or domes and lesser ignimbrites as well as rare scoria, tuff, small intrusives and minor sedimentary rocks;
- comprise at least 80 mappable rock units forming eight discrete domains;
- were probably developed in a continental silicic setting;
- are of subalkaline to mildly alkaline affinity, but contain contradictory petrogenetic indicators and cannot be compared directly with any known magma type or geological setting; and
- are probably products of a complex melt environment that developed through multiple of petrogenetic and geological stages.

Basalts occurring in the volcanic pile at Boggabri are an integral part of the Boggabri Volcanics, and referring them to the Werrie Basalt is impractical.

Structural relationships within the Boggabri Ridge cast doubt on it being a major source of conglomerates in the Maules Creek Formation. Some rhyolite clasts in the Maules Creek Formation contain coarse quartz phenocrysts, but are plagioclase-poor and lack biotite and therefore do not resemble any know rocks from the Boggabri Volcanics. These clasts, and hence possibly all felsic volcanic clasts, might have come from a source other than the Boggabri Volcanics.

Modelling suggests that the source of the Boggabri Volcanics was Fertile MORB Mantle that had been enriched by subduction zone fluids, then depleted during arc volcanism (i.e. leaving both depleted MORB mantle and residual arc signatures) and then re-enriched by addition of a minor nephelinite or carbonatite component (i.e. doubly enriched, doubly depleted). Reactivation of the melt zone of Late Carboniferous arc volcanic rocks during Early Permian crustal extension is a likely cause. The compositional diversity of the Boggabri Volcanics is attributed primarily to fractionation and source heterogeneity, and to limited magma mixing combined with eruptive and depositional processes (e.g., fractionation during ignimbritic eruption, formation of pitchstones), as well as subsequent alteration.

This interpretation differs in detail from all previous models. However, the thermal model of Brownlow (1981a) (see also back-arc basin models cited in Table 8) was reasonably close because the MORB-like basalt petrology is consistent with 'embryonic sea-floor spreading'. While that model requires refinement — for example, a model involving peridotite diapirs ascending to the lower lithosphere, then mafic melts segregating and intruding the extending lithosphere as dykes (Tatsumi and Eggins, 1995) — is more likely than a model involving mafic or ultramafic diapirs intruding the lower crust, its outright rejection by Scheibner (1993) on petrological grounds was clearly premature.

Finally, there is ample scope for additional field and laboratory investigations of the Boggabri Volcanics. Priority should be placed on: isotopic investigations to constrain igneous petrogenesis; on comprehensive investigations to validate and fully characterise each mappable rock units recognised herein; on detailed investigations of depositional facies to refine the depositional model and correlations herein; on studies of alteration assemblages to differentiate Early Permian weathering from hydrothermal alteration, and to identify possible mineralised zones; and on radiometric dating to establish the age of the Boggabri Volcanics and to help constrain the Permo-Carboniferous evolution of eastern Australia. In addition, this study has laid a base for detailed reinvestigation of the role of the Boggabri Ridge in subsequent Gunnedah Basin sedimentation. Such investigations should include modelling of the Gunnedah Basin sequence to determine whether:

- the 'string of beads' appearance of the outcrops of the Boggabri Ridge reflects interference between longitudinal and transverse folds;
- the apparent mismatch of transverse folds across the Boggabri Ridge (Fig. 3) could reflect tear faulting along the Boggabri Fault;
- tear faulting and interference folding together could provide a mechanism to source the Porcupine Formation by locally reworking the Boggabri Ridge and/or the Maules Creek Formation; and
- the above would be compatible with NW-SE shortening inferred regionally for Porcupine Formation time (see Appendix 5).

# References

Arculus R.J., 1987. The significance of source versus process in the tectonic controls of magma genesis. *Journal of Volcanology and Geothermal Research* **32**, 1–12.

Arculus R.J., 1994. Aspects of magma genesis in arcs. *Lithos* **33**, 189–208.

Arculus R.J. and Gust D.A., 1995. Regional petrology of the San Fransico Volcanic Field, Arizona, USA. *Journal of Petrology* **36**, 827–861.

Arculus R.J., Gust D.A. and Kushiro I., 1991. The evolution of Fuji and Hakone volcanos, Honshu, Japan. *National Geographic Research and Exploration* **7**, 276–309.

Arculus R.J. and Johnson R.W., 1978. Criticism of generalized models for the magmatic evolution of arc-trench systems. *Earth and Planetary Science Letters* **39**, 118–126.

Asthana D. and Leitch E.C., 1985. Petroi Metabasalt: alkaline within-plate mafic rocks from the Nambucca Slate Belt, northeastern New South Wales. *Australian Journal of Earth Sciences* **32**, 261–277.

Bailey J.C., 1981. Geochemical criteria for a refined tectonic discrimination of orogenic andesites. *Chemical Geology* **32**, 139–154.

Basaltic Volcanism Study Project (BVSP), 1981. *Basaltic Volcanism on the Terrestrial Planets.* Pergamon Press, New York, 1286 pp.

Bembrick C.S., Herbert C., Scheibner E. and Stuntz J., 1973. Structural subdivision of the New South Wales portion of the Sydney-Bowen Basin. *Geological Survey of New South Wales, Quarterly Notes* **11**, 1–13.

Bloxham W. and Lewis A.D., 1972. Ti, Zr and Cr in some British pillow lavas and their petrogenetic affinities. *Nature (Physical Science)* **237**, 134–136.

Briggs D.J.C., 1993. Time control in the Permian of the Sydney-Bowen Basin and the New England Orogen. *In* Findlay R.H., Unrug, R., Banks M.R. and Veevers J.J. (eds), *Gondwana Eight: Assembly, Evolution and Dispersal.* A.A. Balkema, Rotterdam, 371–383.

Brown G.E. Jr., 1982. Olivines and silicate spinels. *Reviews in Mineralogy* **5**, 275–381.

Brown R.E., Brownlow J.W. and Krynen J.P., 1992. *Manilla- Narrabri 1:250,000 Metallogenic Map SH/56–9, SH/55–12: Metallogenic Study and Mineral Deposit Data Sheets.* Geological Survey of New South Wales, Department of Mineral Resouraces, Sydney, 319.

Brownlow J.W., 1977b. Stratigraphic subdivision of the Early Permian coal measures in the Boggabri area, and regional implications. *Advances in the Study of the Sydney Basin, 11th Symposium, Department of Geology, University of Newcastle, Abstracts*, p. 19.

Brownlow J.W., 1978. Late Carboniferous and Permian palaeogeography of western New England. *Advances in the Study of the Sydney Basin, 12th Symposium, Department of Geology, University of Newcastle, Abstracts*, pp 20–22.

Brownlow J.W., 1981a. A thermal model for the origin of the Sydney and Gunnedah Basins. *Advances in the Study of the Sydney Basin, 15th Symposium, Department of Geology, University of Newcastle, Abstracts*, 10–12.

Brownlow J.W., 1981b. Early Permian sediments in the Maules Creek district, New South Wales. *Australian Coal Geology* **2**, 125–160.

Brownlow J.W., 1982a. A time space plot through north-eastern New South Wales for the Late Carboniferous – mid Triassic. *In* Flood P.G. and Runnegar B. (eds), *New England Geology, Voisey Symposium*. pp. 179–182. Department of Geology, University of New England, and AHV Club, Armidale.

Brownlow J.W., 1982b. Diapirism and the development of four thermal provinces in north-eastern New South Wales. *In* Flood P.G. and Runnegar B. (eds), *New England Geology, Voisey Symposium*. pp. 229–237. Department of Geology, University of New England, and AHV Club, Armidale.

Brownlow J.W., 1987. The New England connection: correlation and contrast across the Hunter-Mooki Fault System. *Advances in the Study of the Sydney Basin, 21st Symposium, Department of Geology, University of Newcastle, Proceedings*, 179–193.

Brownlow J.W., 1988a. Tectonothermal regimes and the mid-Carboniferous to Middle Triassic evolution of north-eastern New South Wales. *Geological Society of Australia, Abstracts* **21**, 72–73.

Brownlow J.W., 1988b. Plate tectonics and the mid Carboniferous to Middle Triassic evolution of eastern Australia — a re-evaluation. *In* Kleeman J.D. (ed.), *New England Orogen — Tectonics and Metallogenesis*. pp. 172–180. Department of Geology and Geophysics, University of New England, Armidale.

Brownlow J.W., in prep. Extending formal nomenclature for mappable rock units beyond lithstratigraphy: a discussion. Report to the Stratigraphic Nomenclature Committee, Geological Society of Australia.

Brownlow J.W. and Arculus R.J., 1993. The geology and geochemistry of the Boggabri Volcanics — a preliminary account. *In* Flood P.G. and Aitchison J.C. (eds), *New England Orogen, Eastern Australia — NEO '93 Conference*. Department of Geology and Geophysics, University of New England, Armidale, 315–322.

Buddington A.F. and Lindsley D.H., 1964. Iron-titanium oxide minerals and synthetic equivalents. *Journal of Petrology* **5**, 310–357.

Cabanis B. and Lecolle M., 1989. Le diagramme La/10–Y/15–Nb/8: un outil pour la discrimination des series volcaniques et la mise en evidence des processus de melange et/ou de contamination crustale. *CR Academy of Science Series II* **309**, 2023–2029.

Campbell I.H. and Griffiths R.W., 1990. Implications of mantle plume structure for the evolution of flood basalts. *Earth and Planetary Science Letters* **99**, 314–338.

Carey S.W., 1934. The geological structure of the Werrie Basin. *Linnean Society of New South Wales, Proceedings* **59**, 351–374.

Carey S.W., 1935. Note on the Permian sequence in the Werrie Basin, with description of new species of fossil plants. *Linnean Society of New South Wales, Proceedings* **62**, 447–456.

Carey S.W., 1969. Keynote address, tectonic framework of the Sydney Basin. *Advances in the Study of the Sydney Basin, 4th Symposium, Department of Geology, University of Newcastle, Proceedings*, 53–59.

Cas R.A.F. and Wright J.V., 1987. *Volcanic Successions*. Allen and Unwin, London, 466 pp.

Cawood P.A., 1982. Tectonic reconstruction of the New England Fold Belt in the Early Permian: an example of an oblique-slip margin. *In* Flood P.G. and Runnegar B. (eds), *New England Geology, Voisey Symposium*. pp. 25–34. Department of Geology, University of New England, and AHV Club, Armidale.

Chappell B.W. and Bryant C.J., 1994. *New England Batholith Granites Chemical Data*. Department of Geology, Australian National University.

Chappell B.W. and Hergt J.M., 1989. The use of known Fe content as a flux monitor in neutron activation analysis. *Chemical Geology* **78**, 151–158.

Chayes F., 1963. Relative abundance of intermediate members of the oceanic basalt-trachyte association. *Journal of Geophysical Research* **68**, 1519–1534.

Chayes F., 1964. Titania and alumina content of oceanic and circumoceanic basalt. *Journal of Geophysical Research* **69**, 126–131.

Chayes F. and Velde D., 1965. On distinguishing between basaltic lavas of circumoceanic and ocean-island type by means of discriminant functions. *American Journal of Science* **263**, 206–222.

Clague D.A. and Frey F.A., 1982. Petrology and trace element geochemistry of the Honolulu Volcanics, Oahu: implications for the oceanic mantle below Hawaii. *Journal of Petrology* **23**, 447–504.

Claoue-Long J.C., Compston, W., Roberts, J. and Fanning C.M., 1995. Two Carboniferous ages: a comparison of shrimp zircon dating with conventional zircon ages and Ar40/Ar39 Analysis. *SEPM Special Publication* **54**, 3–21.

Coleman R.G., 1977. *Ophiolites*. Springer-Verlag, Berlin, 229 pp.

Collins W.J., Offler R., Farrell T.R. and Landenberger B., 1993. A revised Late Palaeozoic-Early Mesozoic tectonic history for the southern New England Folt Belt. *In* Flood P.G. and Aitchison J.C. (eds), *New England Orogen, Eastern Australia — NEO '93 Conference.* pp. 69–84. Department of Geology and Geophysics, University of New England, Armidale.

Cox K.G., Bell J.D. and Pankhurst R.J., 1979. *The Interpretation of Igneous Rocks.* Unwin Hyman, London, 450 pp.

Crawford A.J., Falloon T.J. and Eggins S., 1987. The origin of island arc high-alumina basalts. *Contributions to Mineralogy and Petrology* **97**, 417–430.

Cuddy R.G., 1978. Internal structures and tectonic setting of part of the New England Batholith and associated volcanic rocks, northern New South Wales. Ph D thesis, University of New England, Armidale, unpublished.

Dawson T.M., 1988. The stratigraphy and sedimentation of a Late Palaeozoic sequence in the Emblem and Quipolly Dome areas, northeast of Quirindi, New South Wales. B.Sc.(Hons) thesis, University of New England, unpublished.

Day R.W., Murray C.G. and Whitaker W.G., 1978. The eastern part of the Tasman Orogenic Zone. *Tectonophysics* **48**, 327–364.

Deer W.A., Howie R.A. and Zussman J., 1992. *An Introduction to the Rock-Forming Minerals.* Longman, Essex, 696 pp.

Degeling P.R. and Runnegar B., 1979. New Early Permian fossil localities at Halls Peak and their regional significance. *Geological Survey of New South Wales Quarterly Notes* **36**, 10–13.

Dirks P.H.G.M., Hand M. Collins W.J. and Offler R., 1992. Structural-metamorphic evolution of the Tia Complex, New England fold belt: thermal overprint of an accretion-subduction complex in a compressional back-arc setting. *Journal of Structural Geology* **14**, 669–688.

Droop G.T.R., 1987. A general equation for estimating $Fe^{3+}$ concentrations in ferromagnesian silicates and oxides from microprobe analyses using stoichiometric criteria. *Mineralogy Magazine* **51**, 431–435.

Duncan A.R., 1987. The Karoo igneous province — a problem area for inferring tectonic setting from basalt geochemistry. *Journal of Volcanology and Geothermal Research* **21**, 13–34.

Emsley J., 1989. *The Elements.* Clarendon Press, Oxford, 251 pp.

Evans P.R., 1967. Review of the Permian palynology of the Sydney Basin. Bureau of Mineral Resources (Australia), Record 1967/103, unpublished.

Evans P.R., 1980. Geology of the Galilee Basin. *In* Hendersen R.A. and Stephenson P.J. (eds), *The Geology and Geophysics of Northeastern Australia.* pp. 299–305. Geological Society of Australia, Queensland Division.

Evans P.R. and Roberts J., 1980. Evolution of central eastern Australia during the late Palaeozoic and early Mesozoic. *Journal of the Geological Society of Australia* **26**, 325–340.

Falvey D.A., 1974. The development of continental margins in plate tectonic theory. *Australian Petroleum Exploration Association Journal* **14**, 95–106.

Farrell T.R., 1988. Structural geology and tectonic development of the Wongwibinda Metamorphic Complex. *In* Kleeman J.D. (ed.), *New England Orogen — Tectonics and Metallogenesis*. pp. 117–124. Department of Geology and Geophysics, University of New England, Armidale.

Finlow-Bates T. and Stumpfl E.F., 1981. The behaviour of so-called immobile elements in hydrothermally altered rocks associated with volcanogenic submarine-exhalative ore deposits. *Mineralium Deposita* **16**, 319–328.

Flood P.G. and Aitchison J.C. (eds), 1993. *New England Orogen, Eastern Australia — NEO '93 Conference.* Department of Geology and Geophysics, University of New England, Armidale, 669 pp.

Flood R.H., Craven S.J., Elmes D.C., Preston R.J. and Shaw S.E., 1988. The Warrigundi Igneous Complex: volcanic centres for the Werrie Basalt New South Wales. *In* Kleeman J.D. (ed.), *New England Orogen — Tectonics and Metallogenesis*. pp. 166–171. Department of Geology and Geophysics, University of New England, Armidale.

Floyd P.A., 1991. Oceanic islands and seamounts. *In* Floyd P.A. (ed.), *Oceanic Basalts*. pp. 174–218. Blackie and Son Ltd., London.

Floyd P.A. and Winchester J.A., 1975. Magma-type and tectonic setting discrimination using immobile elements. *Earth and Planetary Scientific Letters* **27**, 211–218.

Gill J.B., 1981. *Orogenic Andesites and Plate Tectonics*. Springer, Berlin, 358 pp.

Gilligan L.B. and Brownlow J.W. (eds), 1987. *Tamworth-Hastings 1:250,000 Metallogenic Map SH 56–13, SH 56–14: Mineral Deposit Data Sheets and Metallogenic Study.* Geological Survey of New South Wales, Sydney, 438 pp.

Gilligan L.B., Brownlow J.W., Cameron R.G. and Henley H.F., 1992. *Dorrigo-Coffs Harbour 1:250,000 metallogenic map, SH/56-10, 11: Metallogenic Study and Mineral Deposit Data Sheets.* Geological Survey of New South Wales, Sydney, 509 pp.

Haggerty S.E., 1976. Opaque minerals in terrestrial igneous rocks. *In* Oxide Minerals, *Short Course Notes* **3**. Mineralogy Society of America, Hg101–300.

Hamilton D.S., 1993. Genetic stratigraphic framework. *In* Tadros N.Z. (ed.), The Gunnedah Basin, New South Wales. pp. 145–163. *Geological Survey of New South Wales, Memoir Geology* **12**.

Hanlon F.N., 1949a. Geology of the North-Western Coalfield. Part IV. Geology of the Gunnedah-Curlewis district. *Royal Society of New South Wales, Journal and Proceedings* **82**, 241–250.

Hanlon F.N., 1949b. Geology of the North-Western Coalfield: Part VI. Geology of the south-western part of County Nandewar. *Royal Society of New South Wales, Journal and Proceedings* **82**, 255–261.

Hanlon F.N., 1950. Geology of the North-Western Coalfield: Part VII. Geology of the Boggabri district. *Royal Society of New South Wales, Journal and Proceedings* **82**, 297–301.

Harrington H.J. and Korsch R.J., 1985. Tectonic model for the Devonian to the middle Permian of the New England Orogen. *Australian Journal of Earth Sciences* 32, 163–179.

Harris N.B.W., Pearce J.A. and Tindle A.G., 1986. Geochemical characteristics of collision-zone magmatism. *In* Coward M.P and Reis A.C. (eds), Collison tectonics. *Special Publication of the Geological Society of London* **19**, 67–81.

Hensel H.D., Chappell B.W., Compston W. and McCulloch M.T., 1982. A neodymium and strontium isotopic investigation of granitoids and possible source rocks from New England, eastern Australia. *In* Flood P.G. and Runnegar B. (eds), *New England Geology, Voisey Symposium*. pp. 193–200. Department of Geology, University of New England, and AHV Club, Armidale.

Hensel H.D., McCulloch M.T. and Chappell B.W., 1985. The New England Batholith: constraints on its derivation from Nd and Sr isotopic studies of granitoids and country rocks. *Geochimica et Cosmochimica Acta* **49**, 369–384.

Herbert C., 1980. Depositional development of the Sydney Basin. *In* Herbert C. and Helby R. (eds), A Guide to the Sydney Basin. *Geological Survey of New South Wales, Bulletin* **26**, 11–52.

Hill M.B.L., 1986. Geology of the Deriah Forest area — implications for the structure and stratigraphy of the Gunnedah Basin. *Geological Survey of New South Wales, Quarterly Notes* **62**, 1–16.

Hofmann A., 1988. Chemical differentiation of the Earth: the relationship between mantle, continental crust and oceanic crust. *Earth and Planetary Science Letters* **90**, 297–314.

Hole M.J., Saunders A.D., Marriner G.F. and Tarney J., 1984. Subduction of pelagic sediments: implications for the origin of Ce-anomalous basalts from the Mariana Islands. *Journal of the Geological Society of London* **141**, 453–472.

Hughes C.J. and Hussey E.M., 1976. Standardized procedure for presenting corrected $Fe_2O_3/FeO$ ratios in analyses of fine grained mafic rocks. *Neües Jahrbuch fur Mineralogie* **H.12**, 570–572.

International Subcommission on Stratigraphic Classification (H.D. Hedberg [ed.]), 1976. *International Stratigraphic Guide*, New York, John Wiley and Sons, 200 pp.

Irvine T.N. and Baragar W.R.A., 1971. A guide to the chemical classification of the common volcanic rocks. *Canadian Journal of Earth Science* **8**, 523–548.

Jenkins R.B. and Nethery J.E., 1992. The development of Early Permian sequences and hydrothermal alteration in the Myall Syncline, central eastern New South Wales. *Australian Journal of Earth Sciences* 39, 223–237.

Jensen H.I., 1907. The geology of the Nandewar Mountains. *Linnean Society of New South Wales, Proceedings* **32**, 842–914.

Jensen L.S., 1976. A New Cation Plot for Classifying Subalkalic Volcanic Rocks. *Ontario Division of Mines Miscellaneous Papers* 66.

Jensen L.S. and Pyke D.R., 1982. Komatiites in the Ontario portion of the Abitibi belt. *In* Arndt N.T and Nisbet E.G. (eds), *Komatiites*. pp. 147–157. George Allen and Unwin, London.

Johannsen A., 1932. *A Descriptive Petrography of the Igneous Rocks, Volume II The Quartz-Bearing Rocks*. The University of Chicago Press, Chicago, 428 pp.

Kay R.W., 1980. Volcanic arc magmas: implications of a melting-mixing model for element recycling in the crust-upper mantle system. *Journal of Geology* **88**, 497–522.

Kenny E.J., 1964. Geological survey of the Coonabarabran-Gunnedah district with special reference to the occurrence of sub-surface water. *Geological Survey of New South Wales, Mineral Resources* **40**, 70 pp.

Kersting A.B. and Arculus R.J., 1994. Klyuchevskoy Volcano, Kamchatka, Russia: the role of high-flux recharged, tapped, and fractionated magma chamber(s) in the genesis of high-$Al_2O_3$ from high-MgO basalt. *Journal of Petrology* **35**, 1–41.

Kleeman J.D., 1982. The anatomy of a tin mineralising A-type granite. *In* Flood P.G. and Runnegar B. (eds), *New England Geology, Voisey Symposium*. pp. 327–334. Department of Geology, University of New England, and AHV Club, Armidale.

Kontos N.A., 1984. Lithofacies analysis of the Early Permian Maules Creek Formation, Gunnedah Basin. B.Sc.(Hons) thesis, University of New England, Armidale, unpublished.

Korsch R.J., 1982. Early Permian tectonic events. *In* Flood P.G. and Runnegar B. (eds), *New England Geology, Voisey Symposium*. pp. 35–42. Department of Geology, University of New England, and AHV Club, Armidale.

Korsch R.J., Wake-Dyster K.D. and Johnstone D.W., 1993. The Gunnedah Basin — New England Orogen deep seismic reflection profile: implications for New England tectonics. *In* Flood P.G. and Aitchison J.C. (eds), *New England Orogen, Eastern Australia — NEO '93 Conference*. pp. 85–100. Department of Geology and Geophysics, University of New England, Armidale.

Kuno H., 1960. High-alumina basalt. *Journal of Petrology* **1**, 121–145.

Kuno H., 1966. Lateral variation of basalt magma types across continental margins and island arcs. *Bulletin of Volcanology* **29**, 195–222.

Le Maitre R.W., Bateman P., Dudek A.. Keller, J., Lameyre, J., Le Bas M.J., Sabine P.A., Schmid R., Sorensen H., Streckeisen A., Woolley A.R. and Zanettin B., 1989. *A Classification of Igneous Rocks and Glossary of Terms.* Blackwell, Oxford, 193 pp.

Le Roux A.P., 1986. Geochemical correlation between southern African kimberlites and South Atlantic hotspots. *Nature* **324**, 243–245.

Lechler P.J. and Desilets M.O., 1987. A review of the use of loss on ignition as a measurement of total volatiles in whole rock analysis. *Chemical Geology* **63**, 341–344.

Leitch E.C., 1993. The floor of the Gunnedah Basin north of the Liverpool Range. *In* Tadros N.Z. (ed.), The Gunnedah Basin, New South Wales. pp. 335–348. *Geological Survey of New South Wales, Memoir Geology* **12.**

Leitch E.C., Morris P.A. and Hamilton D.S., 1988. The nature and tectonic significance of Early Permian volcanic rocks from the Gunnedah Basin and the southern part of the New England Fold Belt. *Advances in the Study of the Sydney Basin, 22nd Symposium, Department of Geology, University of Newcastle, Abstracts*, 9–15.

Leitch E.C. and Skilbeck C.G., 1991. Early Permian volcanism and Early Permian facies belts at the base of the Gunnedah Basin, in the northern Sydney Basin and in the southern part of the New England Fold Belt. *Advances in the Study of the Sydney Basin, 25th Symposium, Department of Geology, University of Newcastle, Proceedings.* 59–64.

Lindsley D.H., 1976. Experimental studies of oxide minerals. *Reviews in Mineralogy* **3**, L61–88.

Loughnan F.C., 1969. *Chemical Weathering of the Silicate Minerals.* American Elsevier Publishing Company, Inc., New York.

Loughnan F.C., 1975. Correlatives of the Greta Coal Measures in the Hunter Valley and Gunnedah Basin, New South Wales. *Journal of the Geological Society of Australia* **22**, 243–253.

Loughnan F.C. and See G.T., 1959. Bentonite and Fullers earth deposits of New South Wales: I. Occurrence, mineralogy and physical properties. *Australasian Institute of Mining and Metallurgy, Proceedings* **190**, 85–104.

MacDonald G.A. and Katsura T., 1964. Chemical composition of Hawaiian lavas. *Journal of Petrology* **5**, 82–133.

MacKenzie W.S., Donaldson C.H. and Guilford C., 1982. *Atlas of Igneous Rocks and Their Textures.* Longman, Essex, 148 pp.

MacLean W.H., 1990. Mass change calculations in altered rock series. *Mineralium Deposita* **25**, 44–49.

Mahood G. and Hildreth W., 1983. Large partition coefficients for trace elements in high-silica rhyolites. *Geochimica et Cosmochimica Acta* **47**, 11–30.

Manser W., 1960. The Geology of the Curlewis-Gunnedah-Boggabri areas. M.Sc.(Prelim) thesis, University of New England, Armidale, unpublished.

Manser W., 1965a. *Geological Map of New England 1:100,000, Curlewis Sheet (No. 330) with Marginal Text.* Department of Geology and Geophysics, University of New England, Armidale.

Manser W., 1965b. *Geological Map of New England 1:100,000, Gunnedah Sheet (No. 320) with Marginal Text.* Department of Geology and Geophysics, University of New England, Armidale.

Mayne S.J., Nicholas E., Bigg-Wither A.L., Rasidi J.S. and Raine M.J., 1974. Geology of the Sydney Basin — a review. *Bureau of Mineral Resources (Australia), Bulletin* **149**, 229 pp.

McDonough W.F. and Sun S.S., 1995. The composition of the Earth. *Chermical Geology* **120**, 223–253.

McKenzie D.E., 1987. Geology, petrology, and tectonic significance of Permian and Carboniferous igneous rocks of the western Georgetown Inlier, north Queensland. *BMR Journal of Geology and Geophysics* **10**, 109–120.

McMinn A., 1981. Early Permian palynology of a sample from KCC Maules Creek DDH 44. Geological Survey of New South Wales, Report Palynology 1981/14, unpublished, (GS1981/158).

McMinn A., 1982. Early Permian palynology of DM Eulah DDH 1. Geological Survey of New South Wales Report Palynology 1982/06, unpublished, (GS1982/138).

McMinn A., 1993. Palynostratigraphy. *In* Tadros N.Z. (ed.), The Gunnedah Basin, New South Wales. *Geological Survey of New South Wales, Memoir Geology* **12**, 135–144.

McNevin A.A. and Holmes G.G., 1980. Gemstones 2nd edition. *Geological Survey of New South Wales, Mineral Industry* **18**, 119 pp.

McPhie J., 1984a. Eruption styles and setting of Late Palaeozoic silicic volcanic centres, New England Orogen, northeastern New South Wales. PhD thesis, University of New England, unpublished.

McPhie J., 1984b. Permo-Carboniferous silicic volcanism and palaeogeography on the western edge of the New England Orogen, north-eastern New South Wales. *Australian Journal of Earth Sciences* 31, 133–146.

McPhie J., Doyle M. and Allen R., 1993. *Volcanic Textures; A guide to the interpretation of textures in volcanic rocks.* Centre for Ore Deposit and Exploration Studies, University of Tasmania, Hobart. 196 pp.

Meschede M., 1986. A method of discriminationg between different types of mid-ocean ridge basalts and continental tholeiites with the Nb-Zr-Y diagram. *Chemical Geology* **56**, 207–218.

Middlemost E.A.K., 1975. The basalt clan. *Earth Science Reviews* **11**, 337–364.

Miyashiro A., 1974. Volcanic rock series in island arcs and active continental margins.

*American Journal of Science* **274**, 321–355.

Moody J.D. and Hill M.J., 1956. Wrench fault tectonics. *Geological Society of America Bulletin* **67**, 1207–1246.

Moody T.C., 1991. The geology of the Halls Peak Volcanics: stratigraphy, structure, geochemistry, tectonic aspects and related volcanogenic massive sulphide deposits. B.Sc.(Hons) thesis, University of New England, Armidale, unpublished.

Moody T.C., Ashley P.M. and Flood P.G., 1983. The early Permian Halls Peak Volcanics and associated massive sulphide deposits: implications for the southern New England Orogen. *In* Flood P.G. and Aitchison J.C. (eds), *New England Orogen, Eastern Australia — NEO '93 Conference.* pp. 331–336. Department of Geology and Geophysics, University of New England, Armidale.

Morgan R.M., 1978. Palynology of samples from Amax/B.H.P. Boggabri DDH 1. Geological Survey of New South Wales Report GS 1978/138, unpublished.

Morimoto N., 1988. Nomenclature of pyroxenes. *Mineralogy Magazine* **52**, 535–50.

Mullen E.D., 1983. $MnO/TiO_2/P_2O_5$: a minor element discriminant for basaltic rocks of oceanic environments and its implications for petrogenesis. *Earth and Planetary Science Letters* **62**, 53–62.

Murray C.G., 1990. Tectonic evolution and metallogeny of the Bowen Basin. *Bowen Basin Symposium, Geological Society of Australia, Queensland Division, Proceedings*, 201–212.

Murray C.G., Fergusson C.L., Flood P.G., Whitaker W.G. and Korsch R.J., 1987. Plate tectonic model for the Carboniferous evolution of the New England Fold Belt. *Australian Journal of Earth Sciences* **34**, 213–236.

Murray C.G., Schneibner, E. and Walker R.N., 1989. Regional geological interpretation of a digital coloured residual Bouguer gravity image of eastern Australia with a wavelength cut-off of 250 km. *Australian Journal of Earth Sciences* **36**, 423–449.

Nockolds S.R. and Allen R., 1953. The geochemistry of some igneous rock series. *Geochimica et Cosmochimica Acta I* **4**, 105–142.

Norrish K. and Hutton J.T., 1969. An accurate X-ray spectrographic method for the analysis of a wide range of geological samples. *Geochimica et Cosmochimica Acta* **33**, 431–453.

Pearce J.A., 1980. Geochemical evidence for the genesis and eruptive setting of lavas from Tethyan ophiolites. *Proceedings of the International Ophiolite Symposium, Cyprus 1979.* pp. 261–272. Institute of Mining and Metallurgy.

Pearce J.A. and Cann J.R., 1971. Ophiolite origin investigated by discriminant analysis using Ti, Zr and Y. *Earth and Planetary Science Letters* **12**, 339–349.

Pearce J.A. and Cann J.R., 1973. Tectonic steeing of basic volcanic rocks determined using trace element analyses. *Earth and Planetary Science Letters* **19**, 290–300.

Pearce J.A. and Gale G.H., 1977. Identification of ore-deposition environment from trace element geochemistry of associated igneous host rocks. *Geological Society of London Special Publication* **7**, 14–24.

Pearce J.A., 1982. Trace element characteristics of lavas from destructive plate boundaries. pp. 525–548. *In* Thorpe R.S. (ed.), *Andesites*. Wiley, Chichester.

Pearce J.A., 1983. Role of sub-continental lithosphere in magma genesis at active continental margins. *In* Hawkesworth C.J. and M.J. Norry (eds), *Continental Basalts and Mantle Xenoliths*. pp. 230–249. Shiva, Nantwich.

Pearce J.A., Harris N.B.W. and Tindle A.G., 1984. Trace element discrimination diagrams for the tectonic interpretation of granitic rocks. *Journal of Petrology* **25**, 956–983.

Pearce J.A. and Norry M.J., 1979. Petrogenetic implications of Ti, Zr, Y and Nb variations in volcanic rocks. *Contributions to Mineralogy and Petrology* **69**, 33–47.

Pearce J.A. and Parkinson, I.J., 1993. Trace element models for mantle melting: application to volcanic arc petrogenesis. *In* Prichard H.M., Alabaster T., Harris N.B.W and Neary C.R. (eds), Magmatic Processes and Plate Tectonics. *Geological Society Special Publication* **76**, 373–403.

Pearce J.A., Van Der Laan S.R., Arculus R.J., Murton B.J., Ishii T., Peate D.W. and Parkinson I.J., 1992. Boninite and harzburgite from Leg 125 (Bonin-Mariana forearc): a case study of magma genesis during the initial stages of subduction. *In* Fryer P., Pearce J.A. and Stokking L.B. et al., *Proceedings of the ODP Scientific Results* **125**, 623–659.

Pearce T.H., Gorman B.E. and Birkett T.C., 1975. The $TiO_2$–$K_2O$–$P_2O_5$ diagram: a method of discriminating between oceanic and non-oceanic basalts. *Earth and Planetary Science Letters* **24**, 419–426.

Pearce T.H., Gorman B.E. and Birkett T.C., 1977. The relationship between major element chemistry and tectonic environment of basic and intermediate volcanic rocks. *Earth and Planetary Science Letters* **36**, 121–132.

Peccerillo A. and Taylor S.R., 1976. Geochemistry of Eocene calc-alkaline volcanic rocks from Kastamonu area, northern Turkey. *Contributions to Mineralogy and Petrology* **58**, 63–81.

Raggatt H.G., 1924. Asbestos, emery, fluorspar, fuller's earth, graphite, phosphates, talc, and soapstone. *Geological Survey of New South Wales, Bulletin* **14**, 15–18.

Reed S.J.B., 1996. *Electron Microprobe Analysis and Scanning Electron Microscopy in Geology*. Cambridge University Press, Cambridge, 201 pp.

Ribbe P.H. (ed.), 1983. *Feldspar Mineralogy, Reviews in Mineralogy* **2**, 2nd Edition, Mineralogy Society of America, 362 pp.

Ringwood A.E., 1975. *Composition and Petrology of the Earth's Mantle*. McGraw-Hill, New York, 618 pp.

Roberts J., Claoue-Long J., Jones P.J. and Foster C.B., 1995. SHRIMP zircon age control of

Gondwanan sequences in Late Carboniferous and Early Permian Australia. *In* Dunay R.E. and Hailwood E.A. (eds), Non-biostratigraphical Methods of Dating and Correlation. *Geological Society Special Publication* **89**, 145–174.

Roberts J., Engel B. and Chapman, J., 1991. *Geology of the Camberwell, Dungog, and Bulahdelah 1:100,000 Sheets, 9133, 9233, 9333.* Geological Survey of New South Wales, Sydney, 382 pp.

Roberts J., Lennox P.G. and Offler R., 1993. The geological development of the Hastings Terrane — a displaced fore-arc fragments of the Tamworth Belt. *In* Flood P.G. and Aitchison J.C. (eds), *New England Orogen, Eastern Australia — NEO '93 Conference.* pp. 231–242. Department of Geology and Geophysics, University of New England, Armidale.

Rollinson H.R., 1993. *Using Geochemical Data: Evaluation, Presentation, Interpretation.* Longman Scientific and Technical, Essex, 352 pp.

Russell T.G., 1981. Stratigraphy and structure of the Gunnedah Basin — a preliminary report. Geological Survey of New South Wales Report GS 1981/045, unpublished.

Saunders A.D. and Tarney J., 1991. Back-arc basins. *In* Floyd P.A. (ed.), *Oceanic Basalts.* pp. 219–263. Blackie and Son Ltd., London.

Saint Smith E.C., 1912. Report on the occurrence of Fullers earth at Boggabri, New South Wales. Department of Mines, New South Wales, Annual Report for 1911, 190–192.

Scheibner E., 1989. The tectonics of New South Wales in the second decade of application of the plate tectonics paradigm, 45th Clarke Memorial Lecture. *Royal Society of New South Wales, Journal and Proceedings* **122**, 33–74.

Scheibner E., 1993. Tectonic Setting. *In* Tadros N.Z. (ed.), The Gunnedah Basin, New South Wales. *Geological Survey of New South Wales, Memoir Geology* **12**, 33–46.

Schmidt B.L., 1988. EL 3076 (Boggabri Project) Boggabri Area, NSW. Geological Survey of New South Wales File GS 1988/259, unpublished.

Shand S.J., 1950. *Eruptive Rocks; Their Genesis, Composition, Classification, and Their Relation to Ore-Deposits.* Thomas Murby and Co., New York, 488 pp.

Shaw S.E. and Flood R.H., 1981. The New England Batholith, eastern Australia: geochemical variations in time and space. *Journal of Geophysical Research* **86**, 10530–10544.

Shaw S.W. and Flood R.H., 1993. Carboniferous magmatic activity in the Lachlan and New England Fold Belts. *In* Flood P.G. and Aitchison J.C. (eds), *New England Orogen, Eastern Australia — NEO '93 Conference.* pp. 113–122. Department of Geology and Geophysics, University of New England, Armidale.

Shaw S.E., Flood R.H. and Langworthy P.J., 1989. Age and association of the Rylstone Volcanics: new isotopic evidence. *Advances in the Study of the Sydney Basin, 23rd Symposium, Department of Geology, University of Newcastle, Abstracts*, 45–51.

Shervais J.W., 1982. Ti-V plots and the petrogenesis of modern and ophiolitic lavas. *Earth and Planetary Science Letters* 59, 101–118.

Shimizu N. and Arculus R.J., 1975. Rare earth element concentrations in a suite of basanitoids and alkali olivine basalts from Grenada, Lesser Antilles. *Contributions to Mineralogy and Petrology* **50**, 231–240.

Sliwa R., Holcombe R.J., Fielding C.R., Little T.A., Bryan S. and Fifoot A., 1993. Early Permian marine fault basins formed during exhumation of the New England Orogen subduction complex in southeastern Queensland. *In* Flood P.G. and Aitchison J.C. (eds), *New England Orogen, Eastern Australia — NEO '93 Conference.* pp. 557–564. Department of Geology and Geophysics, University of New England, Armidale.

Smith J.V., 1974. *Feldspar Minerals. I. Crystal Structure and Physical Properties.* Springer-Verlag, Heidelberg, 627 pp.

Smith J.V., 1983. Some chemical properties of feldspars. *In* Ribbe P.H. (ed.), *Feldspar Mineralogy, Reviews in Mineralogy* 2, 2nd Edition, Mineralogy Society of America, pp. 281–296.

Smith R.L., 1960. Zones and zonal variations in welded ash flows. *USGS Professional Papers* **354F**, 149–159.

Sparks R.S.J., Self S. and Walker G.P.L., 1973. Products of ignimbrite eruptions. *Geology* 1, 115–118.

Spencer E.W., 1969. *Introduction to the Structure of the Earth.* McGraw-Hill, New York, 597 pp.

Stanton R.L., 1994. *Ore Elements in Arc Lavas.* Clarendon Press, Oxford, 391 pp.

Statham P.J., 1995. Quantifying benefits of resolution and count rate in EDX microanalysis. *In* Williams D., Goldstein J. and Newbury D. (eds), *X-Ray Spectrometry in Electron Beam Instruments.* pp. 101–126. Plenum Press, New York.

Stevens B.P.J. and Willis I.L., 1983. Systematic classification of rock units: a key to mapping and interpretation of the Willyama Compex. *In* Stevens B.P.J. and Stroud W.J. (eds), Rocks of the Broken Hill Block: their classification, nature, stratigraphic distribution and origin. pp. 1–56. *Geological Survey of New South Wales, Records* **21**.

Stolz A.J., 1983. *The Nandewar Volcano.* Ph D thesis, University of New England, Armidale, unpublished.

Sun S.S. and McDonough W.F., 1989. Chemical and isotopic systematics of oceanic basalts: implications for mantle composition and processes. *In* Saunders A.D. and Norry M.J. (eds), Magmatism in the Ocean Basins. *Geological Society of London Special Publication* **42**, 315–345.

Sylvester P.J., 1989. Post-collisional alkaline granites. *Journal of Geology* **97**, 261–280.

Tadros N.Z. (ed.), 1993a. The Gunnedah Basin, New South Wales. *Geological Survey of New South Wales, Memoir Geology* **12**, 649 pp.

Tadros N.Z., 1993b. Structural elements. *In* Tadros N.Z. (ed.), The Gunnedah Basin, New South Wales. pp. 55–86. *Geological Survey of New South Wales, Memoir Geology* **12**.

Tadros N.Z., 1993c. Lithostratigraphy. *In* Tadros N.Z. (ed.), The Gunnedah Basin, New South Wales. pp. 95–134. *Geological Survey of New South Wales, Memoir Geology* **12**.

Tatsumi Y. and Eggins S., 1995. *Subduction Zone Magmatism.* Blackwell, Oxford, 211 pp.

Taylor S.R. and McLennan S.M., 1985 *The Continental Crust: Its Composition and Evolution.* Blackwell, Oxford, 312 pp.

Thirlwall M.F., Upton B.G.J. and Jenkins, C., 1994. Interaction between continental lithosphere and the Iceland Plume—Sr-Nd-Pb isotope geochemistry of Tertiary basalts, NE Greenland. *Journal of Petrology* **35**, 839–879.

Thomson S., 1986. An analysis of Early Permian deposition in the Gunnedah Basin, New South Wales. MSc thesis, University of New England, Armidale.

Thomson S., Skilbeck C.G. and McDonald S.J., 1993. *In* Tadros N.Z. (ed.), The Gunnedah Basin, New South Wales. pp. 169–212. *Geological Survey of New South Wales, Memoir Geology* **12**.

Veevers J.J., Conaghan P.J. and Shaw S E., 1993. Permian and Triassic New England Orogen/Bowen-Gunnedah-Sydney Basin in the context of Gondwanaland and Pangea. *In* Flood P.G. and Aitchison J.C. (eds), *New England Orogen, Eastern Australia — NEO '93 Conference.* pp. 31–52. Department of Geology and Geophysics, University of New England, Armidale.

Vickers M.D., 1991. The Werrie Volcanics, Wingen, NSW: geology, geochemistry and tectonic significance. *Advances in the Study of the Sydney Basin, 25th Symposium, Department of Geology, University of Newcastle, Proceedings*, 51–58.

Vickers M.D., 1993. The Lower Permian Werrie Volcanics: facies and tectonic setting. *In* Flood P.G. and Aitchison J.C. (eds), *New England Orogen, Eastern Australia — NEO '93 Conference.* pp. 323–330. Department of Geology and Geophysics, University of New England, Armidale.

Voisey A.H., 1964. *Geological Map of New England 1:100,000, Boggabri Sheet (No. 310), with marginal text.* Department of Geology and Geophysics, University of New England, Armidale.

Walker G.P.L., 1971. Compound and simple lava flows and flood basalts. *Bulletin of Volcanology* **35**, 579–590.

Weaver B.L., 1991. The origin of ocean island basalt end-member compositions: trace element and isotopic constraints. *Earth and Planetary Science Letters* **104**, 381–397.

Wedepohl K.H. (ed.), 1978. *Handbook of Geochemistry.* Springer-Verlag, Berlin.

Whalen J.B., Currie K.L and Chappell B.W., 1987. A-type granites: geochemical characteristics, discrimination and petrogenesis. *Contributions to Mineralogy and*

*Petrology* **95**, 407–419.

Wilkinson J.F.G., 1971. The petrology of some vitrophyric calc-alkaline volcanics from the Carboniferous of New South Wales. *Journal of Petrology* **12**, 587–619.

Wilson M., 1989. *Igneous Petrogenesis*. Unwin Hyman, London, 466 pp.

Winchester J.A. and Floyd P.A., 1977. Geochemical discrimination of different magma series and their differential products using immobile elements. *Chemical Geology* **20**, 325–343.

Whitehouse J., 1993. Coal resources of the Maules Creek Sub-basin. *In* Tadros N.Z. (ed.), The Gunnedah Basin, New South Wales. pp. 523–533. *Geological Survey of New South Wales, Memoir Geology* **12**.

Wood D.A., 1980. The application of a Th–Hf–Ta diagram to problems of tectonomagmatic classification and to establishing the nature of crustal contamination of basaltic lavas of the British Tertiary volcanic province. *Earth and Planetary Science Letters* **50**, 11–30.

Wright T.L., 1974. Presentation and interpretation of chemical data for igneous rocks. *Contributions to Mineralogy and Petrology* **48**, 233–248.

Yaxley G.M., Crawford A.J. and Green D.H., 1991. Evidence for carbonatite metasomatism in spinel peridotite xenoliths from western Victoria, Australia. *Earth and Planetary Science Letters* **107**, 305–317.

Yoo E.K., 1988. The Rocky Glen Ridge and Gilgandra Trough, beneath the Surat Basin. *Geological Survey of New South Wales Quarterly Notes* **72**, 17–27.